MSEL

Materials Science and Engineering Laboratory

INTELLIGENT PROCESSING OF MATERIALS

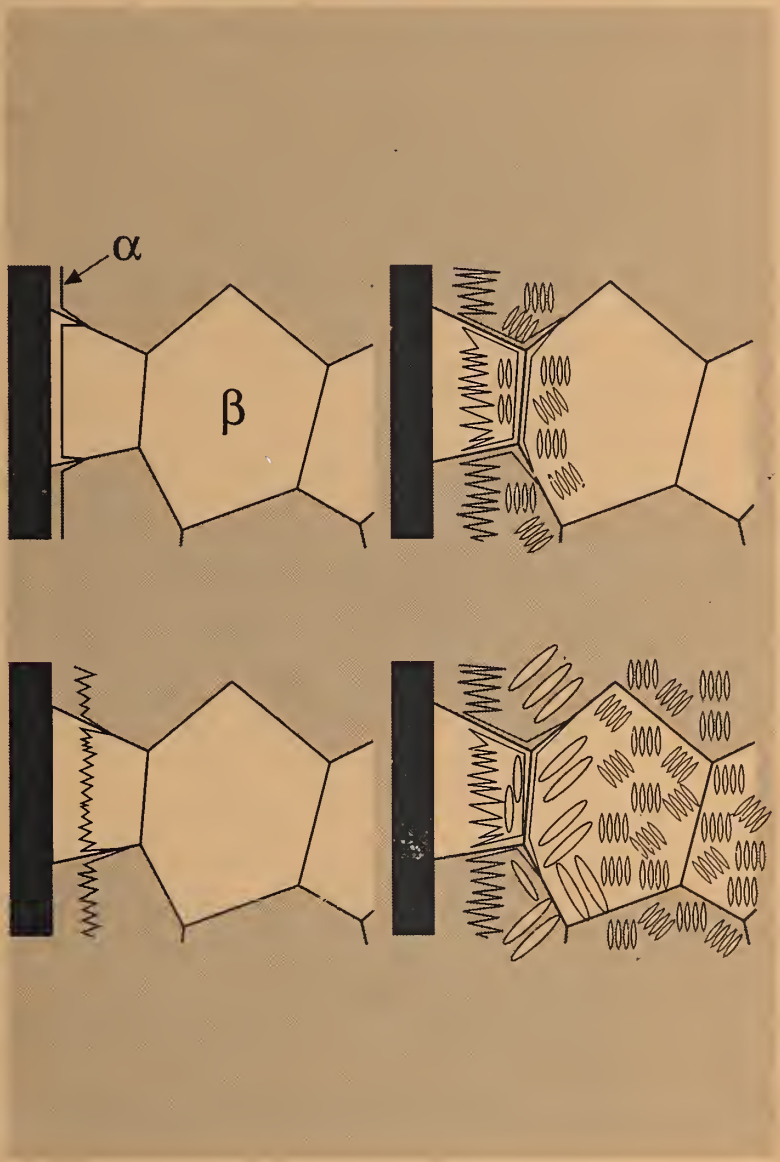

NAS-NRC
Assessment Panel
April 21-22, 1994

NISTIR 5312
U.S. Department of Commerce
Technology Administration
National Institute of Standards
and Technology

Technical Activities 1993

Reaction with the mold wall causes formation of a surface layer of coarse a-phase plates on the surface of titanium aerospace castings. Reliable mechanical performance demands that this layer be removed from the casting surface before use. A theoretical model of the layer formation allows prediction of the thickness which must be removed.

MSEL

Materials Science and Engineering Laboratory

INTELLIGENT PROCESSING OF MATERIALS

H.T. Yolken, Chief
G. Birnbaum, Senior Scientist

NAS-NRC
Assessment Panel
April 21-22, 1994

NISTIR 5312
U.S. Department of Commerce
Technology Administration
National Institute of Standards
and Technology

Technical Activities 1993

U.S. DEPARTMENT OF COMMERCE
Ronald H. Brown, Secretary

TECHNOLOGY ADMINISTRATION
Mary L. Good, Under Secretary for Technology

NATIONAL INSTITUTE OF STANDARDS AND TECHNOLOGY
Arati Prabhakar, Director

Companies and commercial products mentioned in this report are cited to either completely specify a procedure or describe an interaction with NIST. Such mention does not imply endorsement by NIST nor necessarily indicate the best choice for that purpose.

TABLE OF CONTENTS

INTRODUCTION

In 1993, the Office of Intelligent Processing of Materials continued to focus on cooperative programs with industry to establish concepts for intelligent processing of materials. Our research activities involve the elements of intelligent processing which are: the development and validation of process models, development of sensors for on-line process control,and in some cases, integration of these elements with an expert computer control system to demonstrate key aspects of intelligent processing of materials. This approach enhances opportunities to link research in this program with other NIST efforts in materials science and engineering and provides for enhanced interactions with industry.

This year, researchers in the Intelligent Processing of Materials program made a number of significant scientific and technical advances. This report describes these technical advances, along with some plans for future research. Several of the noteworthy advances are highlighted below.

- NIST researchers collaborating with U.S. industry in the NIST Consortium on Intelligent Processing of Rapidly Solidified Metals Powders by High Pressure Gas Atomization have transferred consortium-developed methodology on sensing and fluid dynamics-based process modelling to consortium members. This methodology is crucial for on-line process control and has resulted in cost savings to our industrial members.

- A research program was initiated with the American Iron and Steel Institute to improve steel processing. The two NIST projects are developing process models for the thermomechanical processing of steel and developing magnetic sensors for on-line determination of the mechanical properties of steel sheet. These two projects have made significant progress. Process modeling for the thermomechanical processing of steel was advanced, and research on the on-line magnetic sensor showed that the magnetic properties determined by the sensor correlate closely with the yield strength of the steel.

- NIST and several U.S. companies started a consortium on the processing of polymer blends. The objective of the consortium is to understand and control the processing and kinetics of mixing/demixing. Mixing/demixing is critical in all polymer blends/alloys processing designed to control microstructure and morphology of the final material and its tailored properties. NIST research was expanded and focused this year to support the consortium. The goals of this research are understanding the shear mixing/demixing and phase separation kinetics after cessation of shear, and interfacial modification and control.

- A NIST/industry consortium on casting of aerospace alloys was started this year. This consortium will improve casting quality by using intelligent processing concepts involving process modeling, process sensing, thermophysical properties data, rapid prototyping, model validation and systems integration. This is a distributed research effort with aerospace companies, universities, non-profit laboratories, and federal agencies. The

consortium was started early in 1993 with NIST in-house research carried out in the Metallurgy and Materials Reliability Divisions.

- A NIST/industry consortium on processing of ceramic slurries was started. Colloidal processing of powders for advanced structural ceramics requires stringent control of particle dispersion in liquids. To this end, work was focussed on electrokinetic sonic amplitude (ESA) measurements. Such measurements were made to study the performance of acidimetric-alkalimetric titrations and to determine the powders' isoelectric points (the pH at which the particles are electrically neutral).

In closing, I would like to say that our program on intelligent processing of materials continues to benefit American industry substantially. This Office is positioned to have a major impact on American industry through its research programs, active communication with a broad range of materials processing specialists, and a growing collaboration with industry to transfer elements of intelligent processing to the American factory. Technology dissemination will continue to gain importance in research planning and execution. We are now involved with five different consortia on intelligent processing of materials and have executed over 40 Cooperative Research and Development Agreements (CRADAs) with our partners. We look forward with great enthusiasm to working with producers of advanced metal alloys, the polymers industry, the ceramics industry, and other users and producers of advanced materials. For more information on projects in this report, contact the individual investigators or the Office of Intelligent Processing of Materials, Materials Building, Room B342, National Institute of Standards and Technology, Gaithersburg, Maryland 20899 (301-975-5727).

H. Thomas Yolken, Chief
Office of Intelligent Processing of Materials

Intelligent Processing of Rapidly Solidified Metal Powders by Inert Gas Atomization

S. D. Ridder (301-975-6175) and F. S. Biancaniello
Metallurgy Division, Materials Science and Engineering Laboratory

G. E. Mattingly (301-975-5939) and P. I. Espina
Process Measurements Division, Chemical Science and Technology Laboratory

T. Vorburger (301-975-3493)
Precision Engineering Division, Manufacturing Engineering Laboratory

S. A. Osella (301-975-4263)
Factory Automation Systems Division, Manufacturing Engineering Laboratory

This report summarizes the Fiscal Year 1993 progress of an ongoing research program that began more than eight years ago when metal powder was first produced in the Metallurgy Division's SiGMA system (Supersonic Inert Gas Metal Atomizer). The current program builds on the previous three-year NIST/U.S. industry consortium research program on this process that ended in July 1990. The Phase 2 consortium (outlined in the 1991 IPM annual report) continues with a focus on real-time particle size sensing. This consortium was initiated using cooperative research and development agreements, direct contracts, and/or work requests with Ampal/Metallurg, Crucible Materials Corporation, DOE - Office of Industrial Processes, General Electric Aircraft Engines, Martin Marietta Energy Systems, Inc., and United Technologies - Pratt & Whitney. The overall research goal is to atomize Inconel alloy 625 with expert system control incorporating a particle size feed-back loop. The accomplishment of this goal will result in several subsystems and methodologies that will be made available to consortium members as they reach a usable and/or functional stage of development. Examples of technologies currently available from this program are the Expert Control System Shell (ECSS) code that runs on Macintosh computers, the particle sizing code written in C, and the Computational Fluid Dynamics (CFD) code written in Fortran so as to be portable to most computer systems. These and other technologies have evolved as needed to meet project objectives (updates are continuously available). Focused subject workshops have been used to transfer these technologies to the consortium members. The first of these single-purpose tutorials (on particle sizing) was held during Fiscal Year 1992 at NIST. The second workshop covering the use of the NIST CFD model for solving supersonic gas flows was held June 8-9, 1993.

A Fraunhofer diffraction instrument is used as an in-situ, real-time powder size sensor. As currently configured, this device provides reliable data during each atomization experiment. The instrument produces a collimated HeNe laser beam that passes through a set of view-ports located upstream of the cyclone separators used to remove the metal powder from the process gas. Powder particles passing through the illuminated volume between the view-ports scatter the laser beam at characteristic angles and intensities relative

to their diameters. The scattering data comprise 32 light intensity values, one measuring undiffracted light that is focused through a hole in the detector array panel and onto a centrally located photo diode, and the rest measuring light diffracted to individual semi-circular photo diodes arranged in a "rainbow" pattern across the diffraction plane. Readings are acquired at a 2 Hz sampling rate concurrent with several analog and digital signals from transducers and actuators measuring pressures, temperatures, incandescence of molten metal spray, valve positions, etc. located throughout the process plumbing. The result is a time-accurate signature of the dynamic response of the SiGMA atomizer. In the past fiscal year, modifications were made in the process plumbing upstream of the laser view-ports that improved the homogeneity of the powder-gas mixture and, therefore, reduced signal fluctuations and noise that result from excessive temperature and powder concentration gradients.

Inversion of the in-situ diffraction data from the particle size sensor yields a Particle Size Distribution (PSD). A comparison between Mie scattering and Fraunhofer diffraction theories showed that the added complexity of Mie scattering provided no significant benefit in the inversion results. Other tests using both in-situ and off-line scattering data have verified the currently implemented Fraunhofer theory for determining particle size distributions. Although there are inconsistencies in the comparison of PSD's derived from diffraction and sieving, these can be accounted for by analysis of the powder morphology (the metal powder is not perfectly spherical and most particles have smaller particles attached to their surface). Statistical analysis of the sieve and diffraction PSD's show good correlation between the two techniques and further strengthens confidence in the in-situ diffraction data. Current analysis is aimed at investigating reduced parameter models of the PSD inversion. The motivation for this work derives from several sources. The project goal is to control the atomizer based on the PSD currently being measured. Evaluation of the atomizer output would be dramatically simplified if one or two parameters could be used to describe the PSD versus the current practice of assigning mass percentages to several size classes. Another motivation arises from a fundamental limitation of the diffraction data. Because the 32 light intensity values are not fully independent (adjacent detectors are highly correlated), they will not support an equal number of inverted parameters that describe the PSD. Examples of reduced parameter models now being studied are the PSD mass or volume median diameter ($D_{(v,.5)}$: 50% of the powder mass is less than this diameter) and the Sauter Mean diameter ($D_{[3,2]}$: diameter of sphere with average volume per unit surface area).

To develop a method for determining the liquid metal flow rate, techniques investigated include strain sensors to measure mass change of crucible, inductive core loss, continuous mass sensing with x-rays, and eddy current sensing of metal flow through the metal delivery tube. The strain sensor technique, although simple in design, proved quite complicated to implement for the SiGMA system. The temperature and electromagnetic noise of the induction furnace coil precluded placement of the sensors immediately below the crucible within the melt chamber. The other available location required a compensating measurement for stresses resulting from the gas jet thrust and the differential pressure between the chambers. The combined effects resulted in a signal-to-noise value too low to warrant

further development. The inductive core loss and x-ray sensing of mass within the crucible have not been tested due to lack of funds. The estimated cost of hardware and time is $15K for either technique with no guarantee of success. Current understandings of measurement limitations would place a higher probability of success on the x-ray technique; however, some concern over the use of a radioactive x-ray source in these instruments reduces their attractiveness.

The eddy current technique has received the most attention during the past two years of work on this project. This effort, if successful, will provide a measurement of liquid velocity within the metal delivery tube. The sensor consists of one driver coil between two pickup coils coaxially arranged around a metal flow tube. The driver coil is used to produce a high frequency ($\simeq$ 100 kHz) magnetic field that induces eddy currents in the conducting molten metal within the flow tube. The pickup coils are positioned to sense the magnetic field produced by the eddy currents within the liquid metal. These pickup coils are wired in series opposition to null the output voltage when the liquid is stationary; however, when the liquid moves, the magnetic field produced by the eddy current within the liquid also moves, resulting in a measurable imbalance between the coils proportional to liquid velocity. During this fiscal year a mathematical model was developed that accounts for specific coil designs and velocity profiles within the column of molten metal. An experimental apparatus was constructed that provides a controlled flow of Hg, and several coil designs were tested in an effort to validate the sensor model. Future work will include improving the sensor signal-to-noise ratio, reducing sensor size, and tests to determine signal sensitivity to medium frequency ($\simeq$ 1 kHz) magnetic fields as expected near an induction melting furnace.

Process modeling has also been advanced in several research areas. These include CFD analysis of gas-only supersonic flow in the atomizing jets and liquid-only flow in the delivery tube used to control the flow of molten metal to the gas jets. A mathematical model of the dynamic response of the entire SiGMA apparatus has also been developed. Results of these studies include the gas-only CFD code (mentioned previously regarding focused subject workshops) and the calculation of metal flow rate in real time from sensors that measure gas mass flow rate and chamber temperature. This has led to incorporation of Gas to Metal Ratio (GMR: the ratio of gas mass flow to metal mass flow) into a list of real-time acquired values, and should prove vital to the final control of SiGMA when expert system control of this quantity is implemented. The CFD code has been used by one consortium member to help redesign his commercial metal atomizer, resulting in dramatic cost savings from reduced argon gas consumption.

Guided by CFD results to date, we have made several changes to the atomization system to enhance process control and to aid the modeling efforts. The inert gas back-fill and melt chamber/atomizing chamber differential pressure supply plumbing now includes a gas flow rate sensor and control system that allows the ECSS to control this differential pressure. This added gas flow rate sensor combined with a similar device in the atomizing gas supply will provide needed data for the processing model. A new exhaust system has been completed that incorporates a two-fold increase in capacity as well as ECSS control of the through-put.

The SiGMA atomizer and controller were improved and expanded to incorporate new features to extend the scope of the experimentation on process response. Additional transducers and motor actuators were added to provide more resolution and speed to the control of the pressures within the melting and atomizing chambers. Each chamber is controlled independently to allow control of both the differential pressure between the chambers and the gas jet pressure ratio (the ratio of gas jet exit pressure to the atomizing chamber pressure). The data acquisition rate has been increased to 2 hz and a photo diode was added to time-stamp the start and end of metal flow. Another important addition needed to characterize the SiGMA system was a two-way valve at the bottom of one of the cyclones that allows for sampling the powder product during an operator determined "steady state" period during an atomization experiment. The SiGMA controller consists of a group of software programs and personal computers configured to acquire and store data during a run, as well as a Graphical User Interface (GUI) that provides operator access to the data and actuators within the SiGMA system. The current configuration of the GUI is shown in Figure 1. The software supporting this GUI allows the operator to quickly alter the arrangement, number, and type of graphical information presented on the screen.

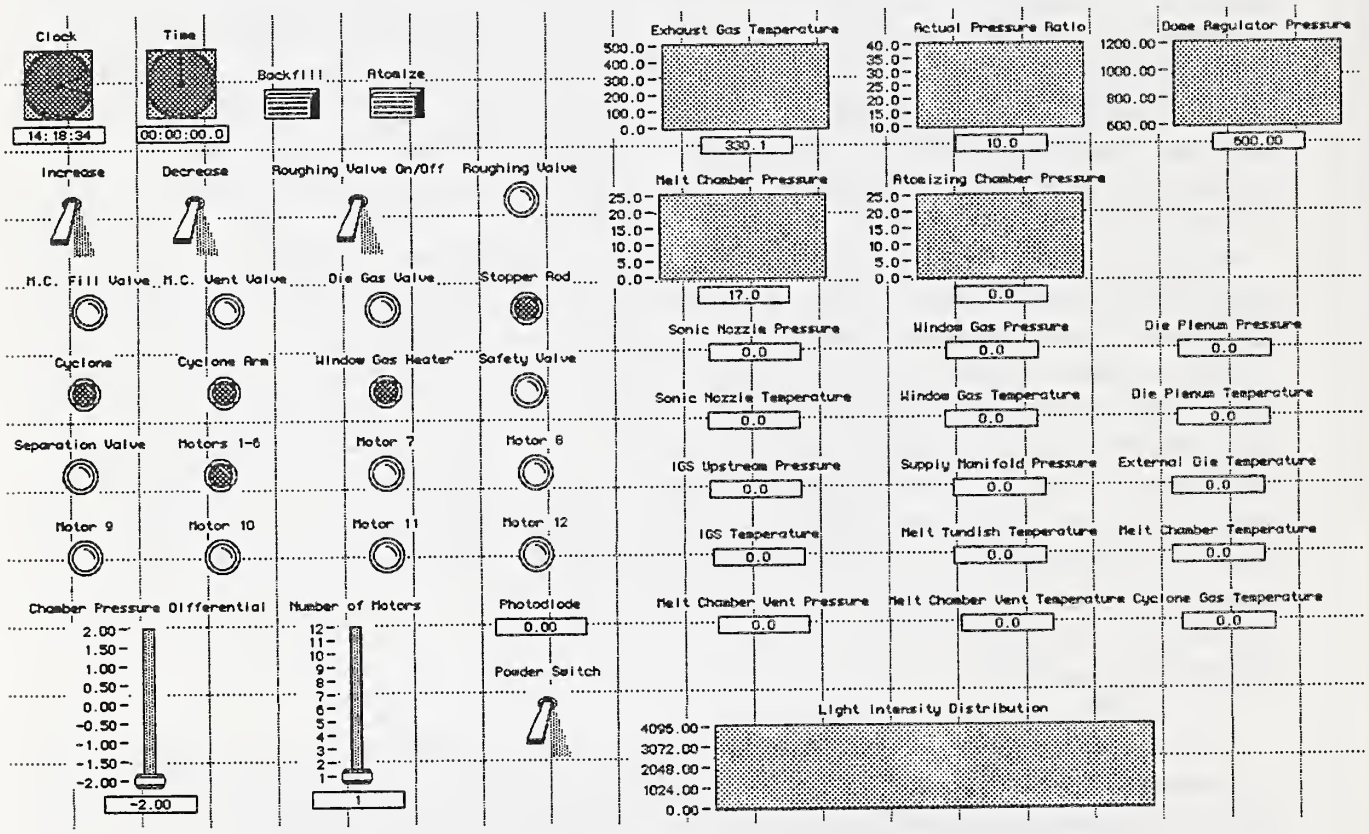

Fig. 1 Graphical User Interface (GUI) of the SiGMA controller. This screen is the primary tool used by the system operator when running the metal atomizer or playing back data acquired during previous atomization runs.

The atomization runs this fiscal year have focused on the completion of a matrix of experiments designed to determine the effect of processing conditions on the resulting PSD. Table 1 outlines this run matrix of 16 experiments consisting of three parameters varied between high and low values. The complete set of runs includes these 16 experiments plus repeats of one of the conditions (number 5) to establish parameter variance. The ***pour temperature*** is the temperature of the molten metal when it leaves the crucible; the ***chamber differential pressure*** is the pressure in the melting chamber minus the pressure in the atomizing chamber (a positive pressure enhances metal flow rate, a negative pressure retards flow); the ***metal delivery tube diameter*** is the diameter of the tube that brings the molten metal into contact with the gas jets; and the ***gas jet pressure ratio*** is the exit pressure of the gas jets divided by the atomizing chamber pressure. These parameters were chosen by a dimensional analysis of the available parameters and consideration of the operating extremes of the SiGMA system. Results to date show a statistical correlation between the gas-to-metal ratio (GMR) and the particle size distribution (PSD) when PSD is represented as either $\mathbf{D}_{(v,.5)}$ or $\mathbf{D}_{[3,2]}$.

Matrix Number	Pour Temperature (°C)	Chamber Differential Pressure (psia)	Metal Delivery Tube Diameter (mm)	Gas Jet Pressure Ratio (dimensionless)
1	1675	+1	2.5	32
2	1675	+1	2.5	43
3	1675	+1	3.0	32
4	1675	+1	3.0	43
5	1675	-1	2.5	32
6	1675	-1	2.5	43
7	1675	-1	3.0	32
8	1675	-1	3.0	43
9	1725	+1	2.5	32
10	1725	+1	2.5	43
11	1725	+1	3.0	32
12	1725	+1	3.0	43
13	1725	-1	2.5	32
14	1725	-1	2.5	43
15	1725	-1	3.0	32
16	1725	-1	3.0	43

Table 1. Experimental Run Matrix

PUBLICATIONS

1. S. D. Ridder, S. A. Osella, P. I. Espina, T. Vorburger, G. E. Mattingly, L. Phillips and F. S. Biancaniello, "NIST/Industrial Consortium on Intelligent Processing of Rapidly Solidified Metal Powders By Inert Gas Atomization," Semi-Annual Report for March 1 to August 31, 1992.

2. S. D. Ridder, S. A. Osella, P. I. Espina, T. Vorburger, G. E. Mattingly, L. Phillips and F. S. Biancaniello, "NIST/Industrial Consortium on Intelligent Processing of Rapidly Solidified Metal Powders By Inert Gas Atomization," Second Annual Report for March 1, 1992 to February 28, 1993.

Casting of Aerospace Alloys

W. J. Boettinger (301-975-6160), A. Cezairliyan, L. Phillips, A. Kahn, and R. J. Schaefer
Metallurgy Division, Materials Science and Engineering Laboratory

T. A. Siewert (303-497-3523)
Materials Reliability Division, Materials Science and Engineering Laboratory

B. Murray (301-975-2713)
Applied and Computational Mathematics Division
Computing and Applied Mathematics Laboratory

This project has the objective of bringing together the components of an intelligent processing system for metal casting to improve the efficiency with which cast alloy parts are produced for the aerospace industry. This improved efficiency is to be obtained by reducing the development time for the design of the casting process for new parts and by reducing the incidence of defects in production parts. Replacing the trial-and-error method of casting design with an approach in which detailed computer models are developed, based on accurate knowledge of phase equilibria and thermophysical properties together with sophisticated theories of microstructure development, will greatly accelerate the process of producing a casting with the required properties.

Many of the components of an intelligent processing system have a long history of development either at NIST or in the laboratories of industrial manufacturers or universities. To bring these components together, and to further develop them in directions that will be most useful to a coordinated system, a Consortium on Casting of Aerospace Alloys has been formed via cooperative research and development agreements (CRADAs) between NIST and a number of corporations, universities, and government agencies. The project is a distributed research effort in which work is done by the collaborating organizations as well as at NIST. This report describes mainly the work done at NIST. At present, the strongest interest of the industrial partners in the consortium relates to engine components, especially to the origin of defects in directionally solidified single crystal turbine blades. Therefore, many of the individual projects in this program relate to the alloys from which these blades are made and the origin of defects in such blades.

Work on this program is divided into four categories: micro/macro modeling, process sensors, thermophysical properties data, and validation and calibration. In each of these areas, NIST scientists work with scientists from the collaborating organizations. In the validation and calibration area, the work is done mainly at the facilities of the industrial partners.

The micro/macro modeling work generates models for the development of microstructure within castings. These microstructure models will enhance the macroscopic

mold-filling and heat flow models in ProCAST™, a commercial casting simulation program of consortium member UES, Inc. At present, most models for microstructure development consider only binary alloys or make simple linear approximations to treat systems with a larger number of components. For a realistic analysis of aerospace alloys, the microstructure models require data on phase equilibria that is best obtained from multicomponent phase diagrams. Even though solidification processes lead to solute distributions that are far from equilibrium, it is well established that equilibrium as represented by the phase diagram is an excellent approximation to the conditions on the interface between the alloy liquid and the growing solid. For multicomponent alloys, phase diagram information cannot be presented graphically. For an alloy with (n) components, the composition of each phase is given by the concentration of (n-1) components. The phase diagram information will be made available as a subroutine of code which will return, for a given liquid composition, the liquidus temperature and the composition of the solid phase.

The thermodynamic data required for the operation of the phase diagram subroutine must be obtained by modeling all the ternary subsystems of the alloy of interest. Experience has shown that these can then be extrapolated to the higher order system with good results. For Inconel 718, a widely used superalloy chosen for initial study by the consortium, the Ni-Fe-Cr-Nb quartenary system will be modeled, so four ternary systems must be considered. Only one of these (Ni-Fe-Cr) is available from the literature, but work has begun on the other subsystems. Later in the program the ternary systems involving Al and other elements will be added to the data base to allow treatment of a wider group of superalloys.

In addition to better phase diagram data, theoretical models of microstructure development during directional solidification require a better understanding of the influence of the container shape on dendritic crystal propagation. Most existing models, and most laboratory experiments, consider growth at constant velocity in a simple cylindrical container. However, such studies shed little light on some of the problems that lead to defects during the production of single crystals in more complex shapes such as turbine blades. A study is now in progress on the origin of new grains during directional solidification in molds having variable cross section. Stray grains that were cause for rejection in turbine blades produced by a consortium member have been examined and their geometry and crystallography characterized. These data give clues concerning the mechanisms of generation of the stray grains, such as nucleation or dendrite fragmentation. At the same time, experiments have been started at NIST in which directional solidification of a model Al-Cu system in containers of variable cross section is used to reveal the behavior of dendrites when they grow in the vicinity of mold corners. These experiments are being used in conjunction with modeling of the heat flow to understand the formation of supercooled regions of the melt. Such supercooled regions may promote the development of stray grains by a variety of mechanisms.

A specific microstructural feature for which consortium members need a model is the layer of alpha phase material that forms as a continuous case on the surface of titanium castings due to reaction with oxygen and possibly other elements from the mold. Because

this excessively hard layer must be removed from the casting prior to use, it is important for the foundries to be able to predict its thickness. Experimental analyses and theoretical models of alpha case formation are in progress. Samples of Ti-6Al-4V castings have been examined metallographically for alpha case thickness and microstructure. Because the beta grains in the interior of castings of this alloy also transform to alpha phase upon cooling to room temperature, the alpha case thickness is detectable metallographically only by the variation in alpha plate size. Coarser alpha plates occur in the surface case region. Accurate chemical profiles are sought for all of the elements present in the alpha case region, but measurements of microchemistry are dificult due to overlap of x-ray emission lines.

Modeling studies of alpha case formation have produced two diffusion approaches suitable for arbitrary cooling curves at the surface of the casting. The simple approach treats the concentration of oxygen at the shell interface as a constant. Then the penetration distance of oxygen into the beta phase can be given by a simple integral involving the temperature and the activation energy for diffusion. The second approach uses a time or temperature dependent value for the surface oxygen concentration and also accounts for the motion of the alph-beta interface that propagates from the surface as the casting cools. This model requires the numerical solution of a finite difference problem in time at each point on the surface of the casting where alpha case thickness data is sought.

The foundry industry needs to improve predictive criteria for the formation of microporosity in dendritically solidified castings. Currently, empirical criteria based on local temperature gradients and solidification rates are used to estimate the tendency for porosity to form. A survey of the current literature in the area of computational modeling of convective and diffusive transport in mushy zone solidification indicates the practicality of evaluating these criteria using relatively large-scale numerical modeling to calculate the flow field, local pressure drop, and temperature field. An investigation of the models used in the existing simplified criterion for microporosity formation indicates that improvements can be made in the description (Darcy's law) that it uses to describe flow conditions in the mushy zone. We have begun work in this area as a first step in employing large-scale computational modeling to verify and enhance the simple predictive criteria.

Two process sensor development projects are under way with the goal of monitoring, in real time, the position of the solid-liquid interface during directional solidification. The first of these uses x-rays to penetrate the wall of a mold and image the growing crystal. Figure 1 shows how x-rays of different voltages would be transmitted through mold walls with thicknesses typical of investment castings. Using existing equipment in the laboratory, we have demonstrated that the crystalline front can be detected at potentials that are appropriate for penetrating the mold wall. These experiments have also revealed the requirements for improved detector components having better resolution and higher sensitivity, and these are now being incorporated into the system.

The second sensor project will employ eddy current methods to determine the solid-liquid interface position. The eddy current method is founded upon an observable change in

the electrical resistivity as the alloy is solidified. Several eddy current coils would be placed in the mold so as to monitor the position of the liquid-solid interface as it passes a particular sensor coil position. Samples of specific alloys of interest have been provided by Howmet, and their electrical resistivity properties are now being measured at temperatures up to and above the melting temperature. Preliminary measurements on the first of these alloys indicate a resistivity change large enough to make the eddy current technique viable.

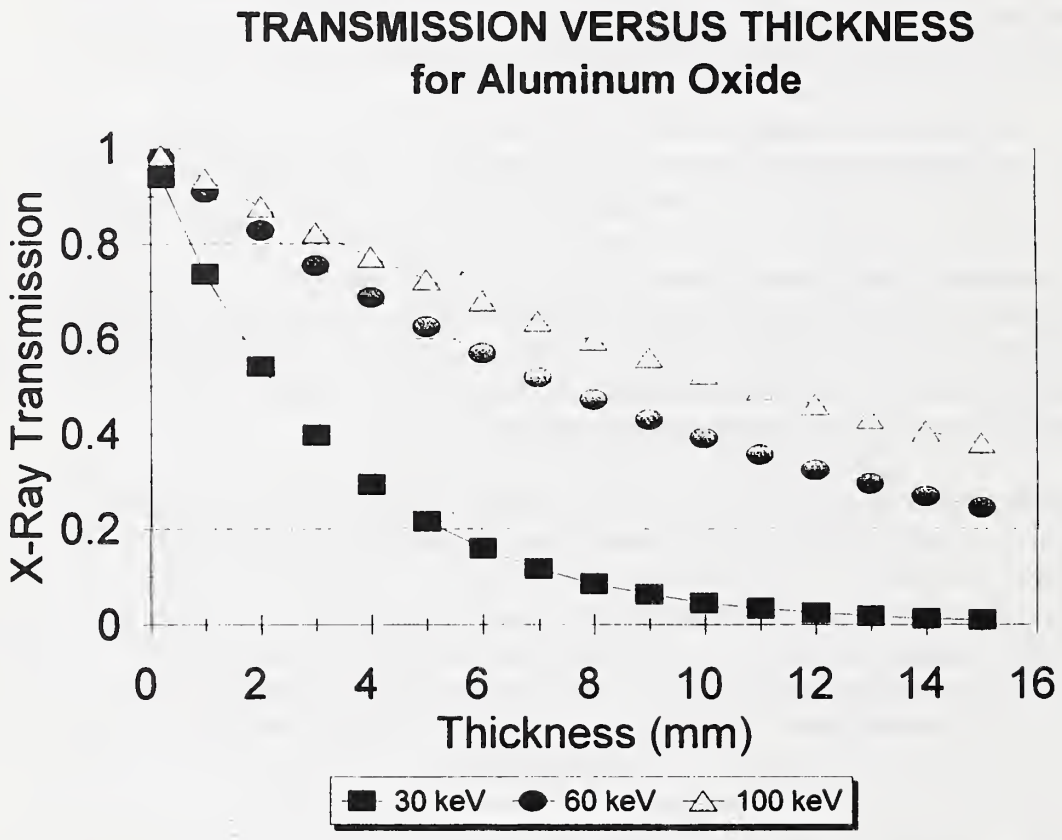

Figure 1. Transmission of x-rays of different voltages through aluminum oxide mold walls.

A critical factor in the development of successful casting process models is the use of reliable thermophysical and related properties data for the specific materials involved in the process. At present, such data are not available for most of the required properties of materials used in aerospace castings. A project is now in progress to obtain properties data on selected aerospace materials in both solid and liquid phases utilizing several experimental techniques and predictive methods. The materials of interest are selected titanium alloys (such as Ti-6Al-4V), Ni alloys (such as Inconel 718), and aluminum alloys (such as A356) and their key constituent elements. NIST and several industrial and academic partners in the casting consortium are contributing to this project.

At NIST, measurements of the heat of fusion, enthalpy, specific heat, and electrical resistivity of liquid nickel up to 2000 K (about 300 K above its melting point) were made using a microsecond-resolution pulse-heating technique. The results, shown in Fig. 2, indicate that above the melting point both enthalpy and electical resistivity increase linearly with temperature, suggesting a constant specific heat for nickel at least up to 2000 K. Nickel, as a key constituent element, was chosen as a test material in preparation for measurements on nickel-based alloys. Similar measurements have begun on Ti-6Al-4V.

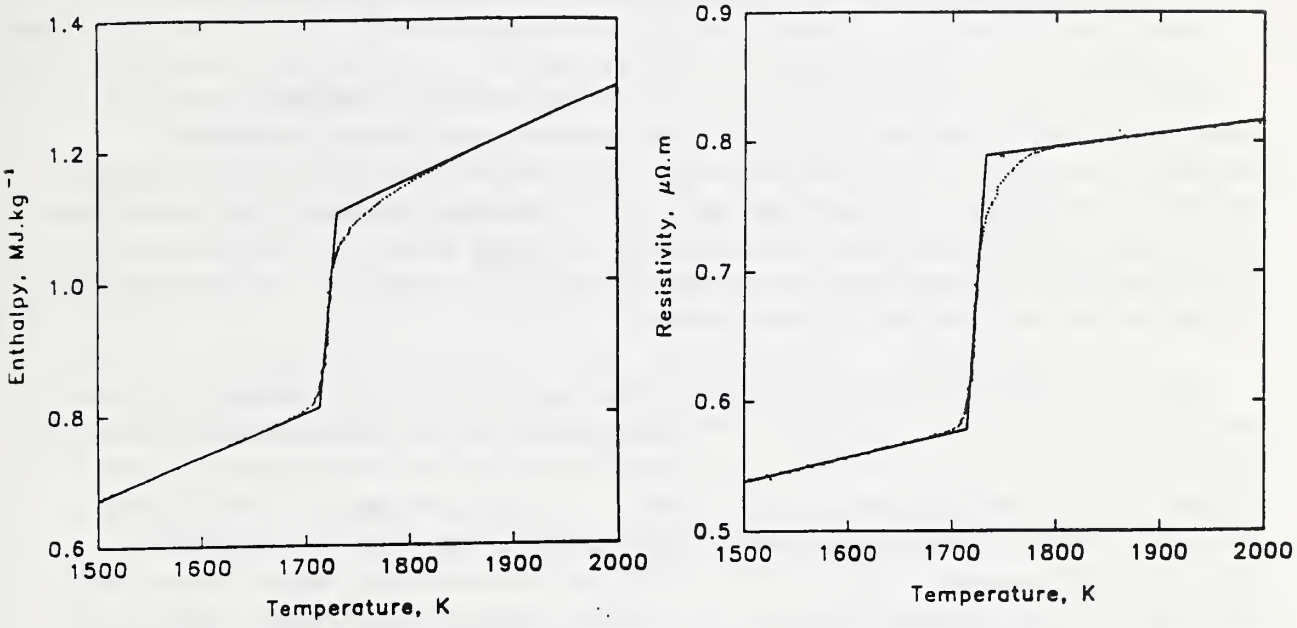

Figure 2. Measured variation of enthalpy (left figure) and electrical resistivity (right figure) of solid and liquid nickel as a function of temperature.

The other consortium members participating in this project have been formulating plans to provide thermophysical properties data on the relevant materials. They will either perform in-house measurements or obtain needed data through contracts with measurement laboratories.

Each of the tasks in this project is being carried out in collaboration with the industrial and academic partners of the casting consortium. Contributions from the partners include providing samples for microstructural analysis or property measurements, making casting equipment available for testing of sensors, pouring fully instrumented castings to validate and calibrate the solidification models, and developing models for specific aspects of casting microstructure. A start-up meeting of the consortium was held on April 8, 1993, and frequent communication occurs on specific projects. Consortium membership, as of October 1, 1993, was 19 organizations in addition to NIST, with others being close to signing.

On-Line, Non-Destructive Mechanical Properties Measurements and Microstructure Engineering in Hot Strip Mills

Y. W. Cheng (303-497-5545) and C. M. McCowan
Materials Reliability, Materials Science and Engineering Laboratory

L. J. Swartzendruber (301-975-6034) and G. E. Hicho
Metallurgy Division, Materials Science and Engineering Laboratory

One of the greatest challenges to the steel-making industry today is the consistent production of large quantities of steel with well-controlled and uniform mechanical properties. For example, consider sheet steel. Approximately 65 million tons of sheet steel per year are produced in the United States. It is estimated that, if the rejection rate of this type of steel could be cut in half, a savings on scrap on the order of $100 million per year could be realized. Production efficiency would also rise due to reductions in the amount of time-consuming and costly testing now required.

NIST is currently collaborating with the American Iron and Steel Institute (AISI) to improve the production of sheet steel. The collaboration currently consists of two major projects. The first project is to develop a predictive tool that can quantitatively link the processing parameters of a hot strip mill to the properties of the hot-rolled steel product. The second project is to develop on-line methods for measurement of the mechanical properties using magnetic methods. Success in these two tasks would enable a steel mill to react quickly when the steel being produced begins to go out of specification, thereby reducing or eliminating scrap and enabling a tighter control of the properties of the steel.

For the first project, the predictive tool will be a user-friendly computer model that incorporates heat flow, knowledge of microstructural phenomena (recrystallization, grain growth, precipitation, and austenite decomposition), and structure-composition-property relationships, to compute the thermal and microstructural evolution of steel during hot rolling, as well as the final product properties, as a function of hot strip mill design and operating practice.

Development of the model will follow well-established principles of microstructural engineering involving computer programming, quantitative characterization of the kinetics of microstructural evolution during hot rolling, measurement of surface heat transfer in the different zones of the hot strip mill, constitutive behavior, and structure-composition-property relationships. The project is a concerted effort of four groups, including NIST, the University of British Columbia (UBC-Canada), US Steel, and Northwest Mettech Corporation (Canada). Major portions of the research will be performed at NIST and UBC. The University of British Columbia will conduct heat-transfer studies, quantitative characterization of kinetics of microstructure evolution, and model verification with plant and pilot-plant trials. NIST's efforts focus on the constitutive behavior and structure-composition-property relationships.

Constitutive equations describe the nonlinear relationship that exists among such process variables as stress, strain rate, and temperature at different deformation levels. For a constant strain, the most commonly used rate equation for hot working is $\dot{\epsilon} = A\ (\sinh\alpha\sigma)^n \exp[-Q/(RT)]$ [1], where $\dot{\epsilon}$ is strain rate, σ is stress, α, n, and A are constants, Q is activation energy for plastic deformation, R is the gas constant, and T is temperature. The constants and the activation energy are functions of chemistry, grain size, dynamic recrystallization, and dynamic precipitation and are determined experimentally. To determine the constants, the activation energy, and the stress-strain behavior at different temperatures and different strain rates, we are using four commercial steels from US Steel. The carbon content ranges from 0.037 to 0.19 % (mass %). Two steels contain microalloying elements, one with 0.08% V and the other with 0.041% Nb.

To date, we have completed a test matrix of 12 conditions with 4 temperatures and 3 strain rates on the two microalloyed steels. The effect of strain rate on stress-strain behavior of the V-treated steel is presented in Fig. 1. The figure shows that true stress increases with increasing strain rate. The figure also shows that true stress increases with true strain and then decreases after reaching a maximum. This phenomenon has not been observed in our previous study of a Nb-treated medium-carbon (0.42%) steel [2]. We believe that the decrease in true stress after reaching a maximum is due to dynamic recrystallization. The stress-strain study has shown the following results:

(1) The amount of true strain required to trigger dynamic recrystallization increases with increasing strain rate, but it decreases with increasing temperature.

(2) At 900 °C with a true strain up to 0.8, the phenomenon of decreasing true stress due to dynamic recrystallization disappeared. It appears that dynamic recrystallization did not occur at these testing conditions.

(3) Dynamic precipitation (precipitation during deformation), has been observed at testing temperatures of 900 and 1000 °C in the Nb-treated steel with a strain rate of 0.2 s^{-1}. This reflects a higher true stress at a lower strain rate; this behavior was only observed in Nb-treated steel. Precipitation of Nb(CN) took place during deformation, resulting in a higher strength at a lower strain rate.

The mechanical properties of a steel, which are important to engineers and users, are closely related to composition and microstructure. Because microstructure and composition of a steel, to a large extent, control the structure-sensitive properties, such as strength, ductility, and strain-hardening characteristics, it is desirable to derive relationships that describe these properties in terms of the microstructural and compositional parameters. The relationships can be used not only to predict the mechanical properties, which are usually obtained from time-consuming destructive testing, but also to optimize the alloy design. For the low-carbon steels, which are the focus of the present project, the strength, ductility (uniform elongation and elongation at fracture), and strain-hardening coefficient are described as functions of composition and ferrite grain size [3,4]. Composition is straightforward and

is determined by alloy design. Ferrite grains are usually assumed to be equiaxed; thus determination of grain size is straightforward. In reality, ferrite grains appear in different morphologies, such as equiaxed, elongated, and acicular. Our efforts to date have been on the characterization of ferrite morphology and inclusion distribution.

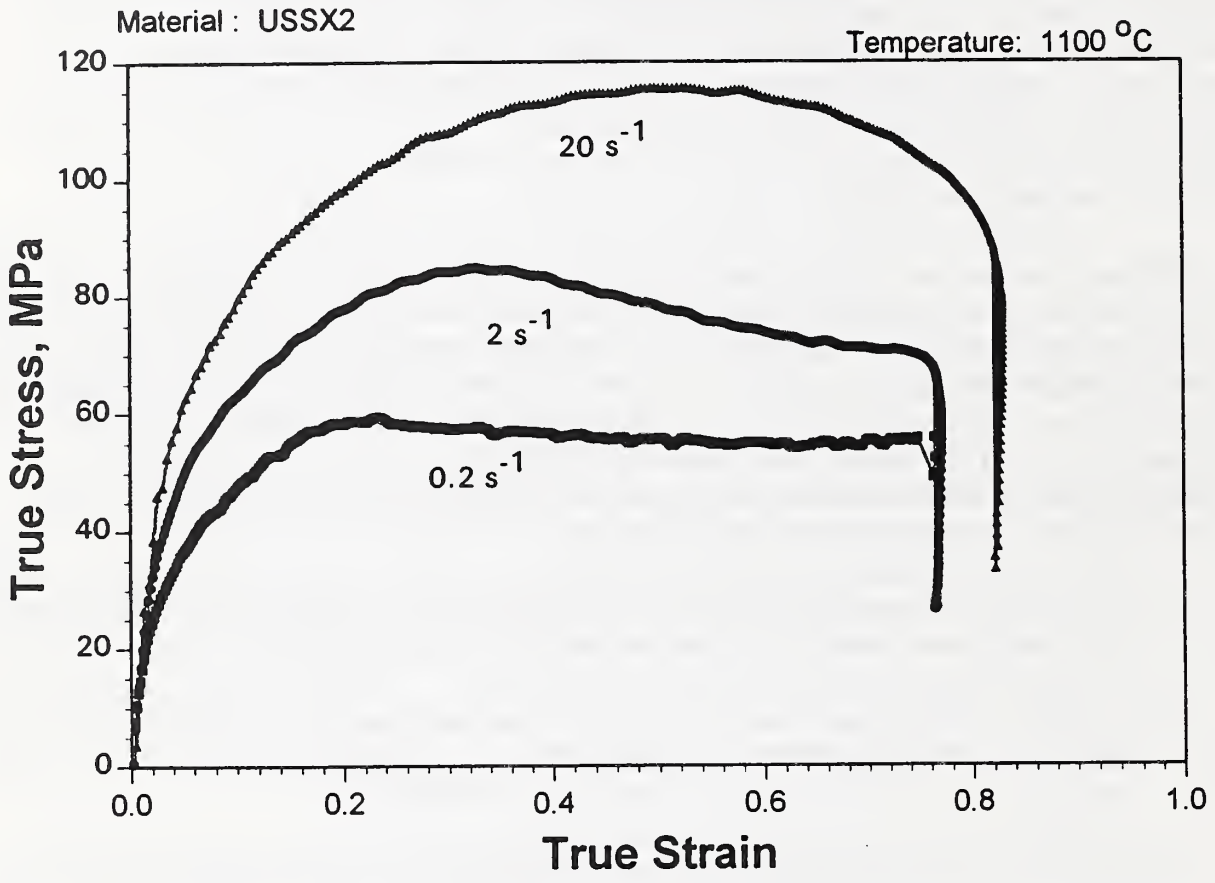

Figure 1. Effects of strain rate on flow behavior of a V-treated low-carbon steel. The figure shows evidence of dynamic recrystallization (decrease of true stress with true strain).

In the two microalloyed steels we have examined, the V-treated steel shows an equiaxed ferrite grain. The majority of ferrite grains in the Nb-treated steel are slightly elongated, but in some areas, the grains appear to be acicular (Fig. 2). We are currently examining the effects of this acicular ferrite on the mechanical properties. Spherical inclusions, containing Ca, O, Mn, Al, and S, are present in both steels. The inclusion content and distribution are similar. The area fraction of inclusions is typically between 0.04 and 0.2%, depending on the sample and location of the measurement. Because of this microstructural nonuniformity, we have developed an image-analysis computer program for quantitative microstructural evaluation in a statistical manner. Each measurement will collect data from 36 different fields. The program is designed to statistically quantify the inclusion content and distribution, pearlite volume fraction, grain size, grain orientation and grain morphology of a steel.

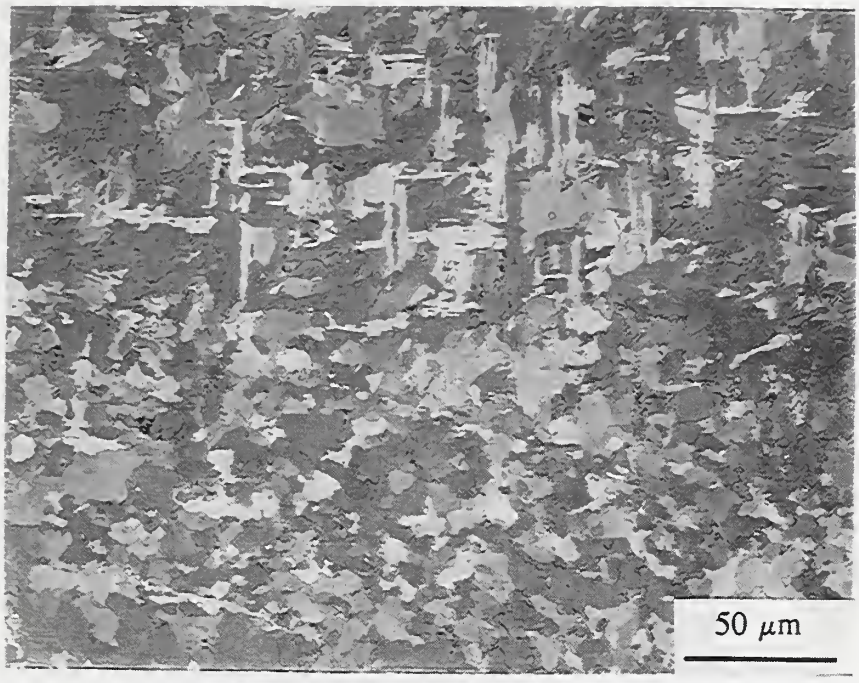

Figure 2. Acicular ferrite of Nb-treated low-carbon steel. Both dark and bright areas are acicular ferrite with different orientations that react differently with the etching reagent.

Our results are transmitted to AISI through monthly progress reports and quarterly reports. As noted above, the mechanical properties of a steel are closely related to composition and microstructure. In the second project, we are attempting to exploit this relationship for on-line measurement of mechanical properties. This project is being carried out in cooperation with LTV Steel Company and Weirton Steel Corporation, who are providing sheet steel samples, and with the Industrial Materials Institute in Canada, who will apply laser ultrasonics to measure grain size. At NIST, we are exploring the use of magnetic methods.

Both the mechanical and the magnetic properties of ferritic sheet steel depend sensitively on the microstructure. Thus magnetic properties may provide a probe for the nondestructive characterization of mechanical properties (see, for example, references 5-6). The magnetic properties, which are sensitive to structure, include initial permeability, maximum permeability, coercive force, remanance, and the Barkhausen effect. Some of these properties, such as coercive force and Barkhausen signal, may lend themselves to rapid on-line measurement as the steel is processed.

In order to be useful, magnetic properties that apply to specific types of steel must be statistically correlated with mechanical properties. Establishing such correlations requires

sets of well-characterized samples that span a range of mechanical properties. The objective is to determine the extent of mechanical property variation for samples within and between representative sheets, and then to determine the same for the magnetic properties. Ultimately, we seek reproducible correlations between a mechanical property, or several mechanical properties, and selected magnetic properties.

To facilitate the rapid testing of the required large number of samples, an automated system consisting of a universal mechanical testing machine, a fast personal computer equipped with analog-digital data acquisition, and programmable high-level software was developed. The data acquisition and analysis procedure consists of four major steps: (1) the test itself, during which instantaneous load and displacement data are acquired at the desired rate and then saved in an ASCII stress-strain data file; (2) determination of the mechanical elastic parameters (Young's modulus, proportional limit) using iterative linear regression; (3) determination of the engineering elastic/plastic and the plastic deformation parameters (0.2% yield stress, ultimate tensile stress, uniform elongation, and elongation at fracture; and (4) evaluation of the true stress-strain, the hardening exponent, the strength coefficient, and the plastic strain ratio (r value). Details of the testing system and evaluation methods are given in reference [7].

For preliminary testing, several sets of sheet steel samples were obtained from a commercial steel mill. Three sheets each from three types of cold-rolled, low-carbon sheet steels were obtained: (1) interstitial free, 1.12 mm thick, coded U-4; (2) interstitial free, Ti stabilized, 0.83 mm thick, coded IF-18; and (3) electrogalvanized, 0.93 mm thick, coded EI-2. Mechanical properties were determined for specimens that were parallel and perpendicular to the rolling direction, and 45° to this direction. Standard ASTM test methods were used to evaluate the mechanical properties of the three different steels. Additional specimens, adjacent to those used for the mechanical property measurements, were sectioned from the sheets and used for the magnetic property measurements. Chemical composition, hardness, and microstructure were also determined for each sheet. Figure 3 shows a summary plot of the average mechanical parameters and their standard deviations obtained for the three steels. Figure 4 shows the coercive force and initial permeability vs. yield stress for this set of samples. Note that the yield stress and coercive force bear a nearly linear relationship, whereas this is not true for the initial permeability.

A variety of sensors and sensor geometries can be used to obtain Barkhausen data including encircling coils, surface pancake coils, and ferrite core surface coils. For on-line measurements, the most practical sensor is a surface coil. The effect of sensor geometry has been stressed in a number of theoretical studies. We have, therefore, compared the nature of the signal obtained from a number of coil geometries. For several low carbon steels with uniform cross sections we found [8] that the shape of the Barkhausen signal was nearly independent of the coil geometry. In particular, the peak signal output occurred at the

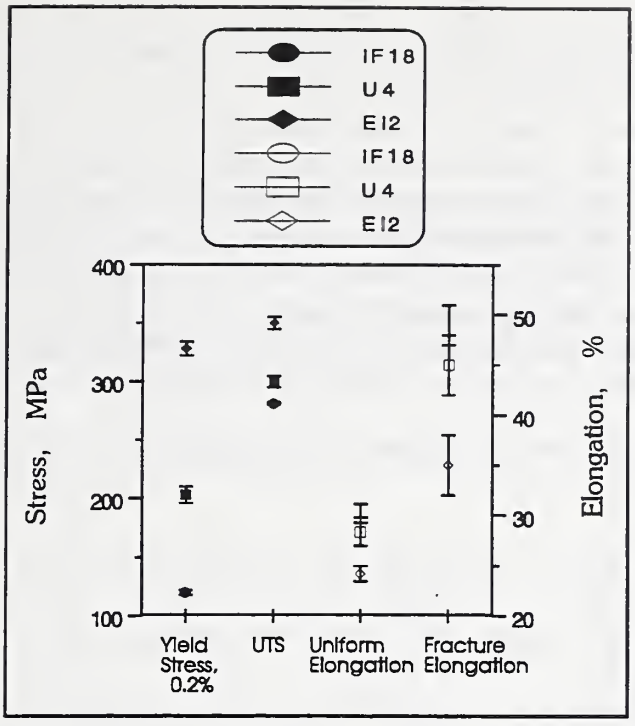

Figure 3. Summary plot of the average mechanical properties and their standard deviations obtained for three low-carbon, cold-rolled sheet steels.

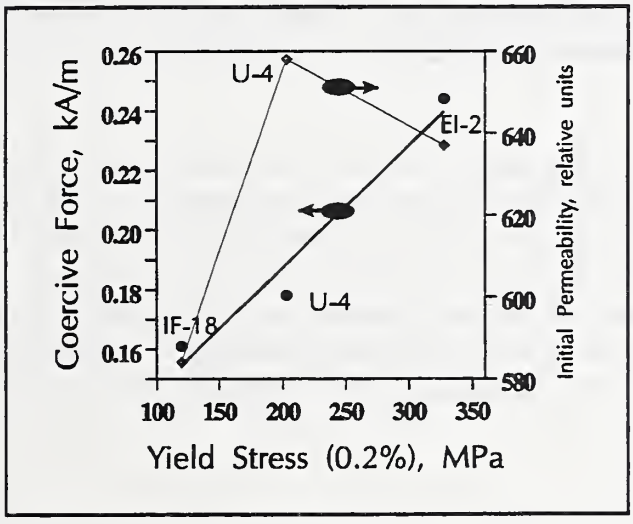

Figure 4. Coercive force (solid line) and initial permeability (dotted line) vs. yield stress for three low-carbon, cold-rolled sheet steels.

same value of tangential field for each coil configuration. This work is being used to help optimize the sensor design for operation at a lift off on the order of 1 mm.

The Barkhausen signals obtained from the three sheet steels, IF-18, U-4, and EI-2, are displayed in Figure 5. Each of the three samples displays a distinctive signal. In particular, sample EI-2 shows two peaks that we attribute to the non-uniform microstructure observed in this sample. The larger peak at lower field is attributed to the surface layer, and the smaller peak at higher field to the bulk of the material. The signal from the surface layer (approximately 10% of the sample) is larger because the contribution to the Barkhausen signal falls off with depth into the sample. This sample is being further investigated by etching layers off the surface and by heat treating the sample.

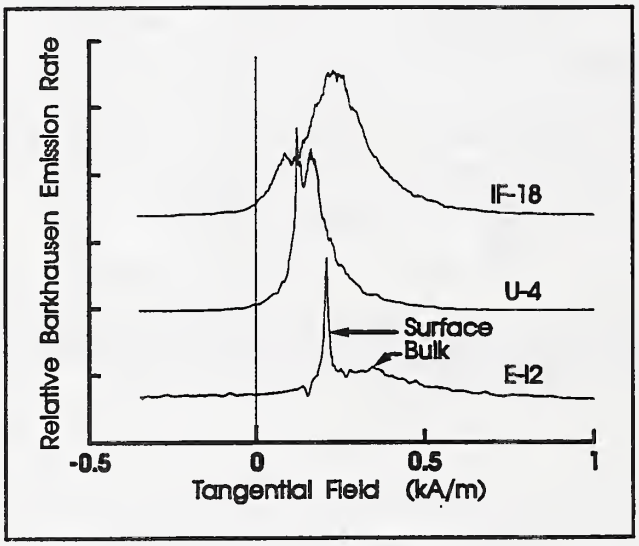

Figure 5. Barkhausen signal emission rates (relative units) vs. tangential magnetic field. The curves have been displaced for clarity.

Phenomonological models that relate the observed Barkhausen signal and other magnetic properties to the domain-wall pinning sites are being explored. We have used [9] an ensemble of stochastic Langevin functions to represent the multiplicity of metastable states with the model parameters being a correlation length, an rms value for the amplitude of the fluctuations in the domain-wall energy gradient, and a "demagnetizing factor." The model was found to generate both hysteresis loops and Barkhausen effect jump size distributions corresponding closely to those observed in the cold-rolled, low-carbon material.

REFERENCES

1. J. J. Jonas, C. M. Sellars, and W. J. McG. Tegart, Metallurgical Reviews, pp. 1-24, (1969).

2. Y. W. Cheng and R. M. Kuziak, "High-Temperature and High-Strain Rate Flow Behavior of a Nb-Treated Bar Steel," presented at the 33rd Mechanical Working and Steel Processing Conference, Oct. 20-22, 1991, St. Louis, MO.

3. F. B. Pickering, Physical Metallurgy and the Design of Steels, Applied Science Publishers, Ltd., London and New York, 1978.

4. P. D. Hodgson and R. K. Gibbs, ISIJ International, Vol. 32, No. 12 (1992), pp. 1329-1338.

5. R. Ranjan, D. C. Jiles, O. Buck, and R. B. Thompson, J. Appl. Phys. 61, 3199 (1987).

6. I. Altpeter and P. Holler, Review of Progress in Quantitative NDE 9, 1837 (1990).

7. Y. Rosenthal. G. E. Hicho, and L. J. Swartzendruber, "Metallurgical Characterization of Selected Sheet Steels for Prospective Magnetic Properties Correlation," NISTIR 5210, June 1993.

8. L. J. Swartzendruber, Y. Rosenthal, and G. E. Hicho, to be published in the 6th Int. Sym. on Nondestructive Characterization of Materials, June 7-11, 1993.

9. L. J. Swartzendruber and G. E. Hicho, Res. Nondestr. Eval. 5, 41 (1993).

10. R. D. McMichael, L. J. Swartzendruber, and L. H. Bennett, J. Appl. Phys. 73, 5848 (1993).

Sensing, Modeling, and Control of Arc Welding

T. A. Siewert (303-497-3523)
Materials Reliability Division, Materials Science and Engineering Laboratory

Weld automation (robotics) was expected to spread through the welding industry in the 1980's, but it has captured only a small share of the market. One of the major barriers to the broader use of automation in welding is the lack of appropriate sensors and control systems. The skills and other capabilities that a welder develops during apprenticeship (recognizing the features that signal weld quality, detecting the appearance of flaws, and choosing appropriate corrective actions) must be replicated in weld sensor and control systems before automation can spread beyond the simple applications where it is being used now.

This year, we concentrated on broadening our arc sensing capabilities. We integrated a light sensor (photodiode) with our voltage and current sensors to provide more information about the welding arc. The arc light intensity falling on the detector is filtered using a blue band-pass filter with a center wavelength of 440 nm and a half power width of 130 nm. The sensor is calibrated with actual arc length data obtained from video image measurements. Estimated arc length in terms of light intensity and current is obtained from an equation of the form:

$$L_{est} = \frac{D_v - C_0}{C_1 I_A + C_2} \qquad (1)$$

where L_{est} is the estimated arc length, D_v is the arc light intensity detector voltage, I_A is the arc current and C_0, C_1 and C_2 are constants obtained from calibration. The combination of the light sensor with the current sensor allowed us to develop a control system for arc length, and is discussed in more detail in the control section. We are now planning a study of the spectral response of various light sensors and the arc using spectral filters and a monochromator.

We also developed a new user interface for our arc quality sensing system. This interface replaces the binary code sent over serial links when this system was customized for the U.S. Navy. The sensing software was modified for easier installation and lower maintenance (reducing the required computer skills) so even small welding shops will be able to use this technology. Even though the initial contacts have been with larger companies, the plan is to use the experiences with large companies to refine the software so that the users at small companies will have a better product. We expect that the ultimate customers will be welding and manufacturing engineers who want to improve the quality of their welded assemblies or wish to troubleshoot specific problems on welding assembly lines. We

developed demonstration software that was sent to 16 companies. This software executes on any PC-compatible computer and illustrates the operation of the user interface with a 7-minute-long file of weld data taken in our laboratory.

The basic weld sensing technology was awarded U.S. patent 5,221,825 in June 1993. Since the disclosure of this invention, various enhancements have been disclosed and these are now under either internal review or patent review.

The arc model developed at MIT under this program in 1992 was also installed at NIST. The model was used cooperatively by researchers at MIT and NIST to predict the power characteristics in gas metal arc welding (GMAW). We found that the principal voltage drop takes place in the arc, which also constitutes the dominant power dissipation. Within the arc region, the largest voltage drops are from the arc column and the cathode fall; the anode fall and electrode regions are somewhat less significant. The power input to the arc column is found to increase both with increasing current and increasing arc length (hence, the need to measure current and arc light intensity to determine arc length in the sensor described above). The model predicts that the major contribution to droplet detachment is the Lorentz forces. The Lorentz forces increase with an increase in current and a decrease in electrode diameter. The model explained the repelled droplet transfer in helium shielding gas as being due to the mass flow of the gas towards the electrode.

An extension of the one-dimensional melting electrode model developed last year was completed for shielded metal arc (SMA) electrodes. Comparisons to experimental data showed that a two-dimensional model was needed. Work has begun on developing a two-dimensional model for SMA.

This year we developed a system to control the arc length in gas metal arc welding. The arc length is estimated using the combination of a photodiode detector to measure arc light intensity and a Hall-effect current transducer to measure arc current. Figure 1 shows the estimated arc length versus the actual with over 15,000 data points. Ideally all points would lie on the straight line. The correlation coefficient for the data fit to equation (1) is 0.97. The sensor is capable of providing the arc length to within a standard deviation of 0.9 mm, about 12 percent of the average arc length and a precision well within the range appropriate for control.

An adaptive control scheme is used to improve our control of the arc length. The contact tube-to-work distance (CTWD) is assumed constant or is provided by an external sensor, and the arc length is measured using the light and current sensors. The CTWD is the sum of the arc length and electrode extension. Here, arc length is controlled by regulating electrode extension. We used theoretical transfer function models between the electrode extension and the square of the arc current that were previously developed. The parameters in the models depend on the set point (the mean electrode extension, and the mean electrode speed). The gains in a proportional-integral-derivative controller are adjusted to place the closed loop poles of the system at desired locations. The electrode extension is used as

feedback to the controller, but, in addition, the electrode extension and the electrode speed are digitally low-pass filtered. These low-pass filtered values are then assumed to be the set

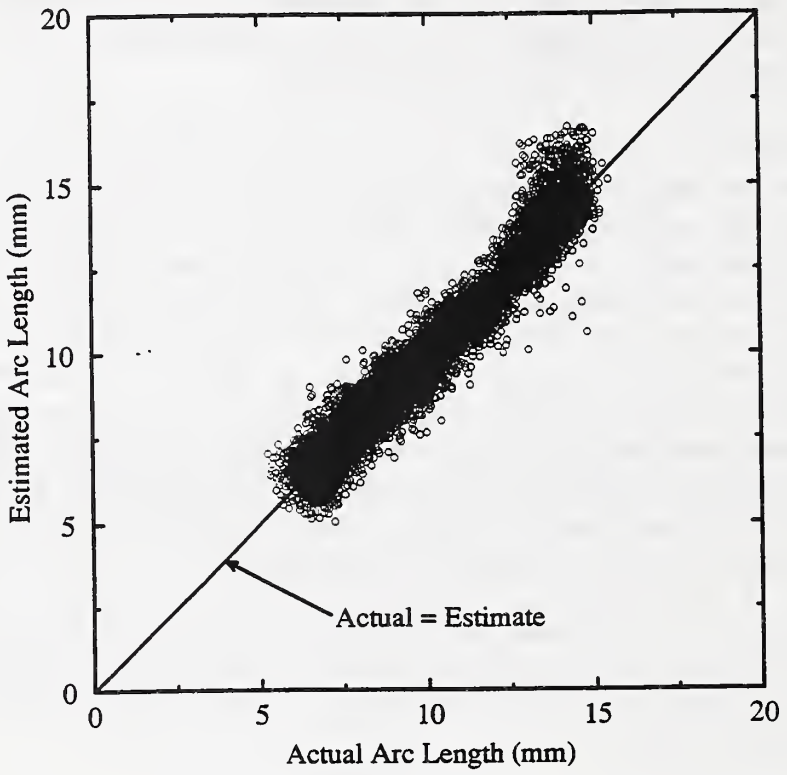

Fig. 1. Comparison of predicted versus measured arc lengths for 15,000 digital images of gas metal arc welding.

point for the transfer function models which results in new model parameters. The gains in the controller are then adjusted to maintain the desired system poles (a form of grain scheduling). The controller was tested and was found to decrease the rise time of the system to a step input in the desired electrode extension by 32% over the uncontrolled case, Fig. 2. The arc length was maintained within 0.8 mm of the set point of 11 mm after 0.6 s for 0.015 m/s step changes in the electrode speed. The desired poles were selected to maximize the response but maintain the current within allowable limits.

To assist in transferring our technology to the welding industry, we packaged it in a way that was easy to implement. We selected an ISA-bus personal computer (IBM-compatible) as the platform, then condensed our sensor algorithms into software written in the C programming language. The result was technology that could be implemented with a hardware cost of less than $4,000 and in a language that was readily supported by industry.

Also, we have developed demonstration software that is sent to interested users. The demo is particularly useful in communicating the technology to young engineers who had been unable to convince their supervisors to authorize travel to our laboratory without some idea of what was available. We organized special sessions at national technical meetings and communicated by phone and letters.

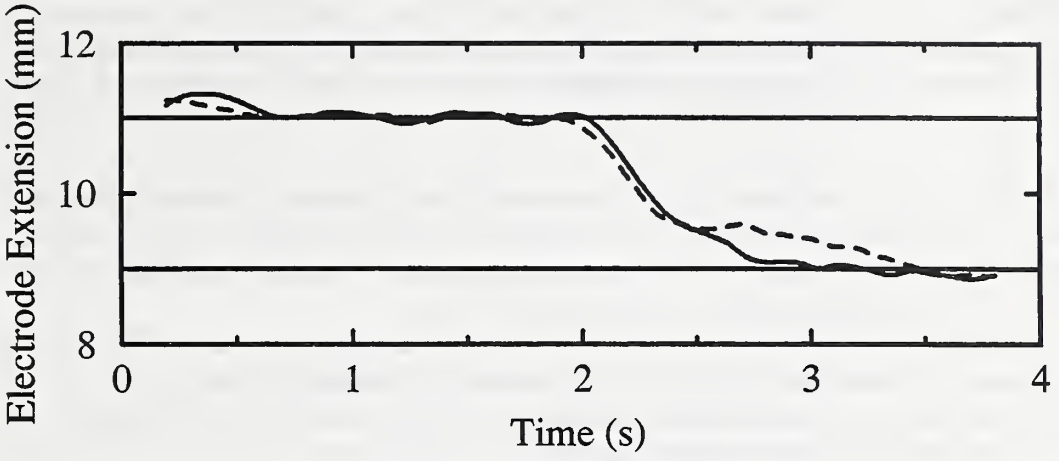

Figure 2. Response of electrode extension to a step change in the contact-tube-to-work distance without control (dotted line) and with control (solid line).

The largest and longest interaction has been with the AC-Rochester Division of General Motors. The interaction began with a visit by GM researchers to the NIST laboratory and led to a CRADA in which the automobile manufacturer sent an engineer to NIST for six months in 1991 to learn the technology. To extend this cooperation for another three years, we signed a second CRADA early in FY93. In this new CRADA, we are providing additional assistance to implement this sensing technology in production and will continue to assist in the interpretation of the data.

To reach potential users of our sensing systems, we organized special sessions on sensing technology at three national technical society conferences this year (the ASM International Fall Conference, the Fourth International Conference on Computerization of Welding Data, and the American Welding Society annual meeting). We also organized and hosted a special conference in September 1993, Commercialization of Advanced Joining Technology Through Industry-Government Partnering to showcase NIST (and other government) welding technology and technology transfer programs.

We made detailed presentations on this technology to 14 potential users this year, some of whom are now evaluating it for their use. A major manufacturer of welding robots plans to use this technology in automating shipyards with intelligent, multifunctional robots. A major welding power source manufacturer plans to use the system to understand the effect of power source design on arc stability and weld spatter characteristics.

REFERENCES

1. T. A. Siewert, R. B. Madigan, T. P. Quinn, and M. Mornis, "Through-the-Arc Sensing for Monitoring Arc Welding Quality in Real Time," Materials Evaluation, 50, p. 1314, November 1992.

2. R. B. Madigan, T. P. Quinn, and T. A. Siewert, "Sensing Droplet Detachment and Electrode Extension for Control of Gas Metal Arc Welding," International Trends in Welding Science and Technology, ASM International, Materials Park, Ohio, p. 999, 1993.

3. T. A. Siewert, R. B. Madigan, T. P. Quinn, and M. A. Mornis, "Through-the-Arc Sensing for Real-Time Measurement of Gas Metal Arc Weld Quality," International Conference on Computerization of Welding Information - IV, ed. T. A. Siewert, American Welding Society, Miami, Florida, 1993.

4. P. G. Jönsson, J. Szekeley, R. T. C. Choo, and T. P. Quinn, "A Survey of Mathematical Models of Arc Welding Processes," 1993, submitted to Modelling and Simulation in Materials Science and Engineering.

5. T. P. Quinn, R. B. Madigan, and T. A. Siewert, "An Electrode Extension Model for Gas Metal Arc Welding," 1992, submitted to the Welding Journal.

6. T. P. Quinn, R. B. Madigan, M. A. Mornis, and T. A. Siewert, "Detection of Wear in Contact Tubes for Gas Metal Arc Welding," 1993, to appear in the Proceedings of the Symposium on Welding and Joining Processes at the 1993 Winter Annual Meeting of the ASME.

7. T. P. Quinn, R. B. Madigan, M. A. Mornis, and T. A. Siewert, "Contact Tube Wear Detection in Gas Metal Arc Welding," 1992, submitted to the Welding Journal.

8. R. B. Madigan, and T. P. Quinn, "Control of Arc Length During Gas Metal Arc Welding Using Arc Light Sensing," 1993, to appear in Proceedings of the International Conference on Modeling and Control of Joining Processes.

9. T. P. Quinn, and R. B. Madigan, "Adaptive Arc Length Controller Design for GMAW," 1993, to appear in Proceedings of the International Conference on Modeling and Control of Joining Processes.

10. P. G. Jönsson, J. Szekely, R. B. Madigan, and T. P. Quinn, "Power Characteristics in GMAW; Experimental and Numerical Investigation," 1993, submitted to the Welding Journal.

Consortium on Intelligent Processing of Powders and Slurries

S. G. Malghan (301-975-6101), P. S. Wang, and V. A. Hackley, Ceramics Division,
and R. Mountain (301-975-2484), Thermophysics Division

The overall goal of this consortium on ceramic powder and slurry characterization is to develop the necessary tools required for intelligent processing of powders/slurries. This will be accomplished through improving our understanding of the surface chemistry of aqueous slurry processing of sintered, reaction-bonded silicon nitride (SRBSN). The focus is on electroacoustic and nuclear magnetic resonance (NMR) techniques. The two primary objectives of this project are described below.

I. Develop the electroacoustic technique to:

a. Identify critical powder parameters affecting electroacoustic measurements
b. Develop interrelationships between powder characteristics and the electroacoustic data
c. Identify the effectiveness of polyelectrolytes as dispersants
d. Develop an on-line measurement capability for electroacoustics. (Figure 1)

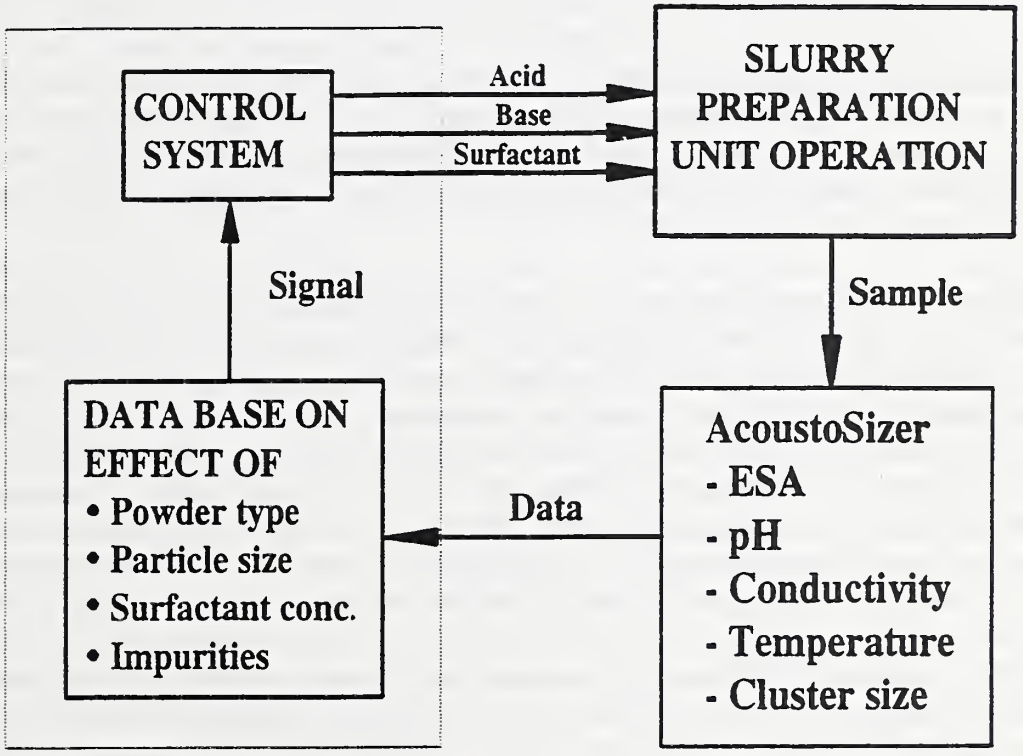

Figure 1. Schematic of (proposed) on-line electrokinetic sonic amplitude (ESA) measurement for intelligent processing of slurries. The results obtained in this program will help us design such a system.

II. Develop and apply NMR spectroscopy and imaging techniques for analysis of powders, slips, and green bodies to provide the following data for processing:

a. Binder distribution in green ceramic,
b. Homogeneity in slurries, and
c. Crystallographic phase/amorphous content characterization

Electroacoustics-- Homogeneity and rheology of powders and slips depends largely on control of reactions at the solid-solution interface. The interfacial electrochemical properties of the slip can be significantly affected by the presence of surface impurities and additives. Electrochemical incompatibility of components may lead to incipient agglomeration and heterogeneity in the green body. Intelligent processing requires a knowledge of component interactions and the potential effects of powder impurities on slip properties. The electroacoustic technique is ideal for studying these interactions in concentrated powder dispersions. In this method a high frequency electrical potential is applied to the suspension. The electrokinetic motion of the particles in the field generates a sound wave whose amplitude is proportional to the particle mobility. The variation of mobility, and the point of zero mobility as a function of suspension pH, yields critical information regarding the surface chemistry of complex multicomponent slips.

Nuclear Magnetic Resonance-- NMR provides an ideal probe to gain insight into microscopic properties of matter by using the weak interaction of nuclear spins with each other and with their environment. The technique uses the difference in the nuclear relaxation time of chemical components in the binder for NMR imaging. Development of various pulse sequences becomes the primary approach for the application of NMR imaging in materials science. Nuclear relaxation is thus one of the most interesting phenomena used to investigate material properties.

A RF-excited nucleus returns to its ground state by releasing energy to crystal lattice and other nuclei. However, in a rigid lattice of a solid, nuclear spin-lattice relaxation (longitudinal relaxation) through the crystal lattice may not occur, resulting in a long nuclear-spin relaxation time (T_1). Rather, the nuclear transverse (spin-spin) relaxation may provide a more effective mechanism for non-equilibrium magnetization decay because of shorter relaxation time, T_2 [1]. Hence, nuclear spin-spin relaxation time becomes a more interesting parameter for solids. In the case of $T_2 << T_1$, as it is in solid samples, T_2 represents the characteristic time for excitation energy to move from one part of the spin system to another. Under this condition, energy put into the spin system will long remain in the spin system, and thus energy diffusion from one region of the spin system to another will occur before dissipation into molecular motion. On the other hand, T_1 becomes short in mobile nuclei (liquid or gas) because of molecular motion and hence nuclear spin-crystal lattice relaxation dominates [2].

We will focus on a few specific issues which provide basic understanding of powder and slurry behavior that can guide processors, and are suitable for adaption to on-line

measurement and control. To provide the basis for on-line particle size measurement and interfacial chemistry control, we plan to take advantage of recent advances in frequency dependent electroacoustic theory and instrumentation made in cooperation with Matec Applied Sciences. Future research will require the design and evaluation of a robust flow-through system for slips that have high solids loading. The measurement of electrokinetic sonic amplitude (ESA) allows the analysis of powder surface chemistry as a function of various parameters in slurries containing in excess of 30% solids by volume. We will investigate the determination of the isoelectric point to characterize the charge behavior of the powder-solution interface, and the interaction of surfactants with other secondary components such as sintering aids.

The unique nature of silicon powder in aqueous environments will be further analyzed through the use of NMR spectroscopy to determine bulk and surface, organic and inorganic impurities. NMR will also be used to ascertain, through the measurement of nuclear spin relaxation times, the nature of adsorption/ desorption interactions in suspensions containing multiple surfactants. These studies, in conjunction with adsorption-desorption isotherms, will provide an understanding of interactions between nonionic polymer and polyelectrolytes.

This report summarizes our FY93 research on silicon nitride and alumina systems by electroacoustics and NMR, respectively. The proposed research on SRBSN will be initiated in September 1993.

Electroacoustics-- For Si_3N_4 the presence of oxygen in the surface region is known to dramatically modify the electrochemical properties. Electroacoustic measurements showed that the isoelectric point of Si_3N_4 decreases linearly with increasing surface oxide thickness [3]. More recently, we characterized the effects of dissolved ions on Si_3N_4 surface chemistry [4], finding that hydrolyzable metal cations, such as Y^{3+}, undergo surface precipitation reactions at the Si_3N_4 surface, which result in metal-hydroxide coatings. Electrochemical and dispersion properties of the coated particles depend on the solubility of the pure hydroxide phase and the hydrolysis constant for the cation. Surface coatings have been used as a chemical means to distribute sintering aids homogeneously and reduce incompatibility problems between components. We have also completed a detailed analysis of ionic contributions to the measured sonic amplitude in the presence of 20 electrolytes [5]. This work provides the necessary information to identify and correct background signals due to the presence of dissolved ions. Under certain conditions these signals can significantly affect the electroacoustic measurement and produce artificial polarity shifts.

Weak-acid polyelectrolytes, such as poly(acrylic acid), are added to slips to control particle dispersion during processing. These polymers impart stability through electrosteric mechanisms which are poorly understood. In the past year, we have investigated the interaction of poly(acrylic acid) with Si_3N_4 using electroacoustic analysis coupled with adsorption measurements and potentiometric titration [6,7]. Work in this area is still in progress; however, preliminary results indicate a complex interaction mechanism between the polyelectrolyte and Si_3N_4 surface. Electroacoustic measurements correlate with adsorption

data as a function of solution pH and polymer concentration. Poly(acrylic acid) adsorbs strongly in acidic medium, where it increases the degree of agglomeration. In alkaline medium, the polyelectrolyte is weakly adsorbed due to repulsive electrostatic interactions. Dispersion properties appear to improve under the latter conditions, suggesting that the free polymer fraction may play a role, not previously considered, in the enhancement of particle stability.

Simulation Studies of Model Aggregates-- A Monte Carlo simulation code was written to generate agglomerates of particles under a variety of conditions. An example of the type of agglomerates produced when the system undergoes phase transition-driven agglomeration is shown in Figure 2. This structure was generated when an initially uniform system with a volume fraction of 20% separated to form agglomerates. The rather open structure is characteristic of many "fractal" agglomerates. The colors indicate the number of near neighbors each particle has in this configuration. The cyan particles have not more than two neighbors, the blue particles have three or four neighbors, and the red particles have up to six neighbors.

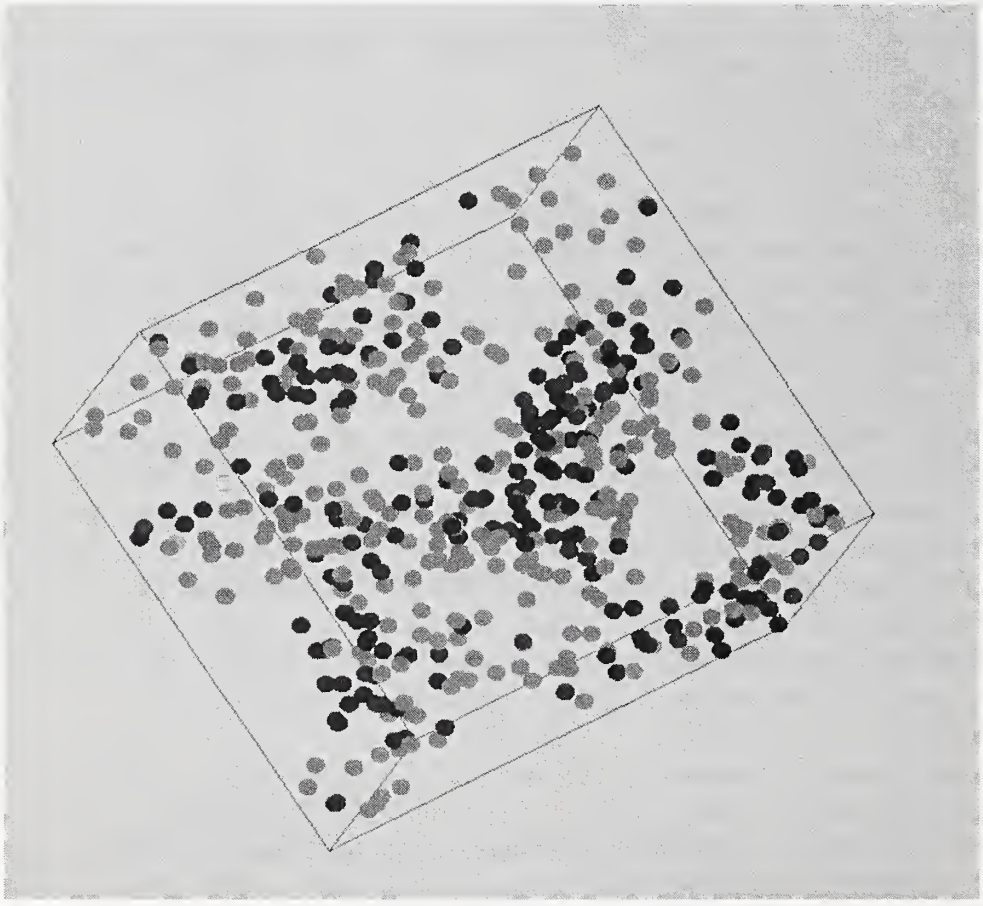

Fig. 2. An example of type of agglomerates produced when the system undergoes phase transition-driven agglomeration.

The aggregation code will be used to generate a spectrum of agglomerates that in turn will be used to simulate the response of agglomerates to the application of frequency dependent, external forces.

NMR-- The nuclear relaxations of organic binders such as wax, stearic acid, and polypropylene, and injection-molded alumina green compacts containing these binders were studied. T_2-weighted NMR imaging technique was developed and applied for the internal mapping of binder distribution [8-10]. The T_2 measurements were performed in a RF-coil of the imaging probe. The ^1H nuclear echo signals were measured by a multiple pulse sequence to construct the three dimensional images.

Block's equations were used to calculate the spin-spin relaxation times from the echo intensities. The T_2 values for paraffin wax and polypropylene were in the 30 to 33 μs range and their intensity decay behaviors were very similar. However, the T_2 value for stearic acid was only 17 μs, and its echo signal intensity decayed more rapidly than those for paraffin wax and polypropylene. Therefore, the measurement of T_2 allows us to detect the presence and variation of different binder contents. Analysis of the molded compacts also showed the presence of a species with a T_2 value near 300 μs. This unexpected species may be the result of a reaction during processing or the presence of moisture. The width of RF-pulses used to measure echoes did not have a significant effect on relaxation times but should be considered in calculation of echo intensities at equilibrium and hence binder composition. This technique development is expected to allow the analysis of both binder content and distribution in molded components with application in process models.

The spatially-resolved, two-dimensional images obtained by application of this technique indicated that the green compacts fabricated from the same nominal binder composition did not have the same content as expected. This observation agrees well with our previous conclusion drawn from nuclear spin echo studies by Hahn's pulse sequence. A 64x64x64 three-dimensional imaging revealed that the binder distribution inhomogeneity and the internal imperfection do exist at certain parts of the samples. A binder-rich folding line, a defect caused by high concentration on binder, was also detected in one of these green compacts.

In the past year, we met with U.S. ceramic industry representatives to seek their ideas on starting a consortium. At this time, five industrial organizations and Oak Ridge National Laboratory have agreed to participate. The initial proposal was revised based on industrial input. The proposed research on sintered reaction bonded silicon nitride was initiated recently.

REFERENCES

1. D. Wolf, Spin-Temperature and Nuclear-Spin Relaxation in Matter: Basic Principles and Applications, Chapter 5, Clarendon Press, Oxford, 1979.

2. R. Lenk, Brownian Motion and Spin Relaxation, Elsevier Scientific Publishing Company, New York, 1977.

3. V. A. Hackley, Pu Sen Wang, and S. G. Malghan, "Effects of Soxhlet Extraction on the Surface Oxide Layer of Silicon Nitride Powders," Mat. Chem. Phys., in press (1993).

4. V. A. Hackley, S. G. Malghan, "The Surface Chemistry of Silicon Nitride in the Presence of Dissolved Ions: Implications for the Effects of Impurities and Additives," J. Mat. Sci., submitted for publication (1993).

5. V. A. Hackley and S. G. Malghan, "Investigation of Parameters and Secondary Components Affecting the Electroacoustic Analysis of Silicon Nitride Powders," in Electroacoustics for Characterization of Particulates in Suspension, NIST Special Publication, in press (1993).

6. V. A. Hackley and S. G. Malghan, "Polyelectrolytes as Dispersants in Colloidal Processing of Silicon Nitride Ceramics," Polymer Preprints, **34**, 1024 (1993).

7. V. A. Hackley, R. S. Premachandran, and S. G. Malghan, "Surface Chemical Interactions of Si_3N_4 with Polyelectrolyte Deflocculants," Materials Forum, to be published.

8. Pu Sen Wang and S. G. Malghan, "Characterization of Si_3N_4 Slurries and Green Bodies by NMR Imaging Technique," to be submitted to Ceramic Bulletin, American Ceramic Society, 1993.

9. Pu Sen Wang, S. G. Malghan, S. J. Dapkunas, K. F. Hens, and R. Raman, "NMR Characterization of Injection Moulded Alumina Green Compacts: II. T_2-Weighted Proton Imaging," submitted to the Journal of Materials Science, 1993.

10. Pu Sen Wang, S. G. Malghan, S. J. Dapkunas, K. F. Hens, and R. Raman, "NMR Characterization of Injection Moulded Alumina Green Compacts: I. Nuclear Spin-Spin Relaxation," submitted to the Journal of Materials Science, 1993.

Consortium on On-Line Sensing for Polymer Processing

Anthony J. Bur (301-975-6748) and Francis W. Wang
Polymers Division, Materials Science and Engineering Laboratory

The goals of this program were established after extensive exchange of information with industry to determine measurement needs which can not be fulfilled using today's technology. Interaction with the polymer processing industry was formalized with the establishment of a NIST/industry consortium, New Measurement Technology for Polymer Processing [1]. This consortium, which is centered at NIST, was initiated on June 1, 1992 and will extend over a period of four years. The members of the consortium are Dow Chemical Co., Rohm and Haas Co., 3M Co., DuPont Co., Flow Vision Inc., and NIST.

The program objective is to develop in-line measurement technology based on optical measurement methods to monitor important polymer processing parameters. Our industrial partners identified the important processing parameters as: shear and extension stress, shear and extension strain rate, non-Newtonian viscosity, temperature, temperature gradients, and the onset temperatures of thermodynamic transitions [1]. The primary optical method employed involves the detection of fluorescence spectra from fluorescent dyes which are doped into the processed polymer material. The character of the fluorescence, i.e. its intensity, polarization, and wavelength distribution, yields information about the state of the polymer matrix. These measurement concepts are applied using optical fibers that are inserted into polymer processing machines at specific positions. In most cases, the optical fiber can be placed into existing instrumentation ports that are normally used for temperature or pressure probes. We demonstrated the measurement method by developing the optical instrumentation to monitor degree of mixing in a twin-screw extruder and to detect the onset of resin solidification during injection molding [2,3].

Over the past year our specific objectives were to initiate the consortium research program, to measure fluorescence anisotropy of rod-like probes under application of shear and extensional stresses, to measure fluorescence decay time and rotational relaxation times of rod-like probes as a function of stress, to evaluate candidate temperature sensitive probes, to design an extensional flow apparatus, and to develop a model for in-situ measurement of extensional strain rate.

Fluorescence Anisotropy Measurements. The physical basis for the sensitivity of fluorescence anisotropy to applied stress is the angular orientation which the dye attains upon extension. This sensitivity is moderated by dependence on fluorescence decay time and rotational relaxation time. In general, the relationship between anisotropy, r, and the state of the dye molecule is

$$r = g(<\cos^2\theta>)/(\tau_f/\tau_r + 1) \qquad (1)$$

where g is a function of the orientation factor $<\cos^2\theta>$, θ is the orientation of the dye dipole moment with respect to the direction of extension, τ_f is the fluorescence decay time, and τ_r is the rotational relaxation time of the dye. The primary effect of applied stress on anisotropy is through the $<\cos^2\theta>$ orientation factor, but τ_f and τ_r can also affect the measurement of r if their ratio is a function of stress.

The measurement of r involves the use of polarized light for excitation and polarization analysis of the resultant fluorescence. In previous work, we used anthracene-tagged polybutadiene as a fluorescent probe doped into a polybutadiene matrix. Anisotropy was found to decrease with increasing shear stress [4]. The difference between the shear and extensional stress effects was examined by developing a model for the relationship between anisotropy, molecular orientation factors, shear stress, and extensional stress [4,5]. An essential requirement for anisotropy sensitivity to shear stress is that the probe molecule engage in the entanglement network of the matrix polymer, i.e. the probe molecule must be macromolecular in size. Thus, under shear stress, the anthracene-tagged polybutadiene probe showed significant change with shear stress, but small fluorescent probe molecules, such as free anthracene and diphenyl hexatriene, which are unable to engage in the molecular entanglement network of the matrix, are insensitive to shear stress.

For extension, we observed that the entanglement requirement does not apply. This is probably because large orientations are possible under extension stress whereas only limited weak orientation occurs under shear stress. Small rod-like fluorescent molecules, such as anthracene and diphenyl hexatriene, which align with the polymer main chain extension, display fluorescence anisotropy change with applied extension stress, but show no significant change with shear stress. The extension observations were carried out using cross-linked polybutadiene. They demonstrate that the rod-like probes can be used to detect the presence of extensional stress in a mixture of extension and shear stress fields. Future extension experiments will be done using polymer melt (uncross-linked) in flow. To do this, we designed an extension flow apparatus with which the flow can be controlled at a constant strain rate.

Measurement of Fluorescence Decay Time and Rotational Relaxation Time. In order to examine the effect of τ_f and τ_r on the measurements of r for stressed polymer systems, we have measured r, τ_f and τ_r as a function of extension for dyes incorporated in a cross-linked polybutadiene matrix. The results show that for moderate extension (up to 150%), there is no significant change in τ_f or τ_r while r changed by 10%, and for higher extensions (up to 300%) the change in the ratio τ_f/τ_r is less than 10%, whereas r changed by 25%. It is clear that the orientation factor, $<\cos^2\theta>$, is the dominant component affecting the anisotropy measurements.

Evaluation of Temperature Sensitive Dyes. Two types of temperature sensitive fluorescent dyes are being used: molecular rotors and excimer-producing dyes. The intensity of fluorescence from these dyes is dependent upon the viscosity and temperature in their molecular neighborhood. One such dye is bis-(pyrene) propane (BPP), which is an excimer-

producing dye and which generates excimer fluorescence at a rate proportional to T/η, where η is a molecular level microviscosity and T is temperature. We used BPP to monitor resin solidification during injection molding [3]. The experimental setup consisted of an optical fiber sensor which was inserted through the wall of the mold and was positioned flush with the mold cavity wall. Excimer fluorescence intensity from polyethylene doped with BPP at a concentration of 10 ppm by weight was measured as a function of time for the mold cycle. When the molten polyethylene resin (200 °C) was injected into the mold held at 55 °C, the resin cooled rapidly and crystallized. The solidification is seen in the data of Fig. 1 which is a plot of excimer fluorescence (normalized) versus time during the cooling phase of the cycle. As the polyethylene cooled, excimer intensity decreased due to the rapid increase in viscosity. A momentary plateau in the intensity after 30 seconds was caused by the heat of crystallization and an elevation of the local temperature experienced by the BPP dye. The data present a view of resin state changes in the mold cavity during the most critical phase of the mold cycle [4,5].

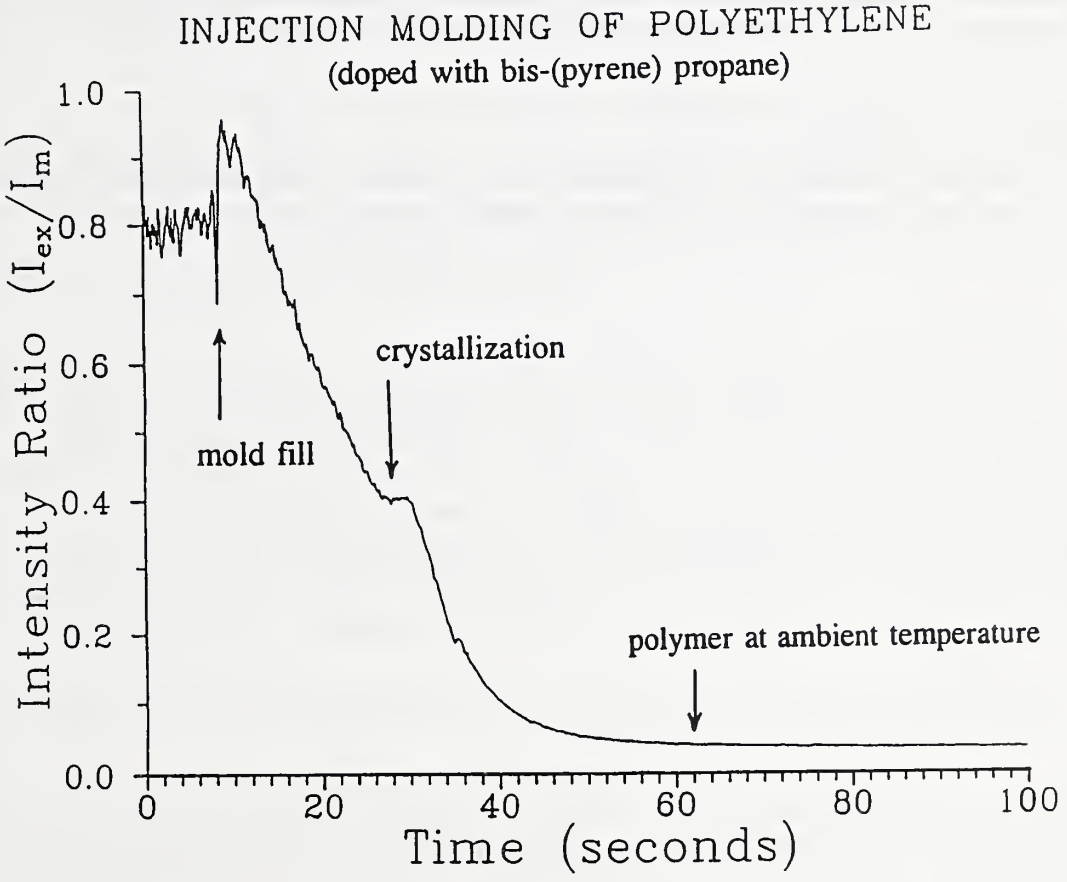

Fig. 1. The normalized excimer fluorescence intensity from BPP doped into polyethylene is plotted versus time for the cooling phase of the injection molding process.

REFERENCES

1. A. J. Bur, P. Handa and C. Grudzien, "Workshop on New Measurement Technology for Polymer Processing," NIST J. Res. 96, 503 (1991).

2. A. J. Bur, and F. M. Gallant, "Fluorescence Monitoring of Twin Screw Extrusion," Polym. Eng. Sci. 31, 1365 (1991).

3. A. J. Bur, F. W. Wang, C. L. Thomas, and J. L. Rose, "In-Line Optical Monitoring of Polymer Injection Molding," Proc. SPE ANTEC Meeting, New Orleans, May 1993.

4. A. J. Bur, R. E. Lowry, S. C. Roth, C. L. Thomas, and F. W. Wang, "Fluorescence Anisotropy Measurements on a Polymer Melt as a Function of Applied Shear Stress," Macromolecules 25, 3503 (1992).

5. A. J. Bur, R. E. Lowry, S. C. Roth, C. L. Thomas, and F. W. Wang, "Fluorescence Anisotropy Measurements on Polymer Materials as a Function of Applied Shear and Extensional Stress," Proc. SPE ANTEC Meeting, Detroit, May 1992.

PUBLICATION

1. A. J. Bur, F. W. Wang, C. L. Thomas, and J. L. Rose, "In-Line Optical Monitoring of Polymer Injection Molding," Proc. SPE ANTEC Meeting, New Orleans, May 1993.

Consortium on the Processing of Polymer Blends

C. C. Han (301-975-6772)
Polymers Division, Materials Science and Engineering Laboratory

The use of polymer blends/alloys has grown in recent years, especially in civilian commerce and consumer products. The growth is primarily due to the low capital investment needed to develop improved properties from existing starting materials. The wide spectrum of properties obtained through the synergistic effect of alloying provides engineering flexibility. The combination of the value enhancement and total sales volume of new polymer blends and alloys in the commercial market leads to enormous added value. The science/technology involved in producing these engineering blends, resins, films, fibers, etc. can be very demanding. The science/technology involved can be summarized to include: (1) thermodynamics of polymer blends; (2) kinetics of phase separation; (3) effects of crosslinking and grafting on the thermodynamics and kinetics; (4) shear mixing/demixing and phase separation kinetics after cessation of shear; (5) interfacial modification and control; (6) simultaneous reaction and phase separation/structure stabilization.

The objective of this effort is to understand the variables controlling the mixing/demixing kinetics. These factors are critical to all polymer blends/alloys processes which are designed to control the structure and morphology of the final material and consequently its tailored properties. The multivariant model inferred from these studies can be used to guide new product development and hopefully in the future will be used as part of an intelligent processing system for on-line control.

Two workshops were held at NIST in April, 1992 and February, 1993 in order to establish dialogue with potential industrial partners and to solicit input from chemical producers. These led to the first consortium meeting on September 24, 1993. At the time of this meeting, five companies (Rohm and Haas, Raychem, 3M, Armstrong World Industry and Aristech) had formally signed agreements to join the consortium, while another eight companies, national laboratory and universities (Lockheed, Allied Signal, Exxon, Goodyear, Sandia National Laboratories, Huron, University of Texas and Stanford University) were in the process of negotiation for joining this consortium.

The direction and immediate tasks have been decided by the Steering Committee as follows:

1. NIST will continue the study of polystyrene/polybutadiene blend system with and without polystyrene-polybutadiene diblock copolymer added as interfacial modifier. This study will serve as the background study, with the participation of industrial partners in order for them to become familiar with various techniques and procedures. In this study, small angle neutron scattering measurements of PS/PB blends at various compositions and containing various concentrations of block copolymers are being carried out. This study will provide

the understanding of the effects of block copolymers on the equilibrium phase behavior. Temperature quench and time resolved light scattering measurements will be carried out in the coming year to study the effect of slowing down of phase separation kinetics due to interfacial modification by block copolymers. The effect of interfacial modification on shear mixing/demixing kinetics and morphology stabilization will also be studied.

2. The Goodyear Tire and Rubber Company is currently carrying out the synthesis of all polybutadienes, polyisoprenes and associated block copolymers for our next study. All consortium partners will fully participate in the study.

3. Exxon is seeking to prepare a polyolefin system for study by the consortium.
The long term strategy of using the laboratory experimental results and accumulated data base in an intelligent materials processing design and control effort will be implemented in several steps:

1. Testing of processing conditions in bench-scale processing equipment based on laboratory experiments.

2. Development of light scattering and video microscopy/image analysis capability for on-line, real time structure determination.

3. System integration and feedback control with either neural networks or other non-linear control tools to supplement the analytical model and laboratory data base.

The current blends consortium effort will be concentrated on the laboratory experimental measurements for up to three blend systems. Existing SANS, Shear SANS, LS and Shear LS instruments will be made available for consortium projects. The new shear light scattering instrument with video microscope detector could become available in the future. Items (1)-(3) will be supported from other project funds if available. However, this could also be the area of the next phase of consortium participation.

Several papers addressing various areas of polymer blends have been published recently by this group (1-10). These include some important and interesting areas relevant to the current consortium project.

REFERENCES

1. "Phase Separation in Deuterated Polycarbonate/Poly-(methylmethacrylate) blend Near Glass Transition Temperature," M. Motowoka, H. Jinnai, T. Hashimoto, Y. Qiu, and C. C. Han, J. Chem. Phys., 99, 2095 (1993).

2. "Dynamic Light Scattering Study of a Diluted Polymer Blend Near Its Critical Point," H. Yajima, D. W. Hair, A. I. Nakatani, J. F. Douglas, and C. C. Han, Phys. Rev. B, 47, 12268 (1993).

3. "Asymptotic Crossover in Polymer Blends," E. K. Hobbie, L. Reed, C. C. Huang, and C. C. Han, Phys. Rev. E, 48, 1579 (1993).

4. "SANS Studies of Space-Time Organization of Structure in Polymer Blends," T. Hashimoto, H. Jinnai, H. Hasegawa, and C. C. Han, International Symposium on Advanced Nuclear Energy Research: Neutrons as Microscopic Probes, March (1993), (in press).

5. "Time Resolved Small-Angle Neutron Scattering Study on Self-Assembling Processes of Deuterated and Protonated Polybutadiene Blends via Spinodal Decomposition: 1. Effect of Initial Thermal Fluctuation," J. Chem. Phys., H. Jinnai, H. Hasegawa, T. Hashimoto, and C. C. Han, (in press).

6. "Shear Induced Morphological Structures in Triblock Copolymers," F. A. Morrison, J. W. Mays, M. Muthukumar, A. I. Nakatani, and C. C. Han, Macromolecules, 26, 5271 (1993).

7. "A Neutron Scattering Study of Shear Induced Turbidity in Polystyrene Dissolved in Dioctyl Phthelate," A. I. Nakatani, J. F. Douglas, Y-B Ban, C. C. Han, J. Chem. Phys. (in review).

8. "Fractal Growth During Early-Stage Spinodal Decomposition in a Hydrogen-Bonded Polymer Blend," E. K. Hobbie, B. J. Bauer, and C. C. Han, Phys. Rev. Lett. (in review).

9. "Structural Stabilization of Phase Separating PC/Polyester Blends Through Interfacial Modification by Transesterification Reaction," H. Yoon, Y. Feng, Y. Qiu, and C. C. Han, J. Polym. Sci., (in review).

10. "Thermodynamic Interactions and Correlations in Mixtures of Two Homopolymers and a Block Copolymer by Small Angle Neutron Scattering," N. P. Balsara, S. V. Jonnalagadda, C. C. Lin, C. C. Han, and R. Krishnamoorti, J. Chem. Phys. (in press).

Ultrasonic Measurements of Near-Surface Damage for Ceramics Process Control

G. V. Blessing (301-975-6627) and J. A. Slotwinski
Automated Production Technology Division, Manufacturing Engineering Laboratory

The objective of this work is to evaluate the capability of ultrasound to nondestructively assess near-surface damage in ceramics caused by surface grinding. Pulsed wave propagation techniques using noncontact sensors are applied to evaluate the material structure. The suitability of these techniques for in-process sensing lends emphasis to their development.

Motivation for this work stems from the manufacturing industry's critical interest in the quality of its ceramic products, especially as they are affected by surface and near-surface structure. This was a recurring theme at the recent International Conference on Machining of Advanced Materials [1]. Grinding damage sites critically influence crack initiation and growth under service stress. The depth of this latent damage may extend from a few to tens of micrometers depending on the material itself, grinding speed, rate of material removal, grit size, and other factors. While rapid grinding with a large grit may be most efficient for part production, a balance must be reached with the residual material damage that may accrue. Reliable techniques for sensing and nondestructively assessing possible material damage are lacking.

Research by us and others (see, e.g., [2]) has demonstrated that high-frequency elastic waves are sensitive to subsurface structure in ceramics. We are pursuing the application of two ultrasonic methods that are feasible for in-process use: the echo amplitude of normal-incident compressional waves, and the amplitude and speed of leaky surface waves. Both methods require a liquid coupling medium between the transducer and material in order to support the high ultrasonic frequencies needed to detect the subsurface structure of interest. For application to in-process sensing, it would be desirable to use the coolant/grinding fluid as the coupling medium.

With the echo-amplitude method, the material displacement generated by normal-incident compressional waves is in the direction of wave propagation, imposing an oscillating pressure perpendicular to the material surface. Near-surface damage affects the echo amplitude of this wave type in at least two ways: (i) an increased material compliance especially due to shallow horizontal cracks, and (ii) phase interference between surface reflections and subsurface reflections. In the leaky wave method, surface waves that are generated by the refraction of incident compressional waves at the Rayleigh critical angle subsequently "leak" their energy back into the liquid coupling medium at the same critical angle. The surface wave has both compressional and shear displacement components as it propagates within the material along the interface. A decrease in the wave amplitude may be attributed to scattering and reflection by cracks and pores. Similarly, a decrease in the wave speed may be attributed to a decrease in material stiffness associated with cracks and pores.

The ultrasonic experimental system consisted of a broadband pulser/receiver, a peak-amplitude detector, and focused transducers operating in the range of 25 to 75 MHz to generate short wave pulses of less than 0.1 μs duration. A majority of the work, including that reported here, was carried out using a 50 MHz transducer possessing an $f/0.8$ spherical lens that produced a measured half-amplitude beam width of about 30 μm in water. The samples were immersed in a room-temperature water bath, and the transducer was attached to a five degree-of-freedom (X, Y, Z, Θ, and Φ) scanning stage. The five degrees of freedom enabled angulation control of the direction (Θ, Φ) of wave propagation for a given transducer position (X, Y, Z). Four of these were motorized for automated line and raster scanning under PC control.

Two types of sample damage were studied this past year: discrete damage sites in glass due to Vickers (pyramidal) indentation, and distributed damage in silicon nitride (Si_3N_4) due to grinding. The discrete-flaw glass sample was studied to provide a reference point for our understanding of the interaction between ultrasound and subsurface cracks [3]. It consisted of a glass slide subjected to a pair of Vickers indents about 50 μm in their diagonal dimension, and separated by 155 μm. Well-understood subsurface cracks were generated, consisting of vertical "half-penny" and "median" cracks with their planes defined by the indent center and corners. Horizontal "lateral" cracks were also generated between the vertical cracks. These lateral cracks occurred at a nominal depth, defined by the indent penetration depth, of 10 to 15 μm for our sample. The optical reflection micrograph in Fig. 1 reveals some of these features. Diametrical segments of the half-penny cracks are visible at the surface, including a prominent segment where they join between proximate corners of the indent pair. By virtue of their subsurface optical reflection, portions of the lateral cracks reveal themselves as bright flares beneath and surrounding the indents.

It is these lateral cracks that we believe are detected and displayed in the echo-amplitude contour plot of Fig. 2 using normal-incident ultrasound. This plot is taken from a raster scan of the glass sample, inclusive of the top indent and the region between the indents. The tightly contoured region in the center of the figure defines the indent location, where the ultrasonic reflection is dominated by the indent topography. Our interest for subsurface damage detection is rather in the surrounding contour regions which are roughly coincident with the flared regions of Fig. 1. Here we observe a reduction in echo amplitude of up to fifteen percent relative to the (undamaged) background level. We interpret this reduction in amplitude as the reflected compressional waves sensing an increased material compliance due to lateral cracking beneath the surface. We note that evidence for the vertical cracks of Fig. 1, with their planes parallel to the incident wave compression, is not discernible in the contour plot of Fig. 2. Their detection would rather require surface-propagating leaky waves incident perpendicular to their crack planes.

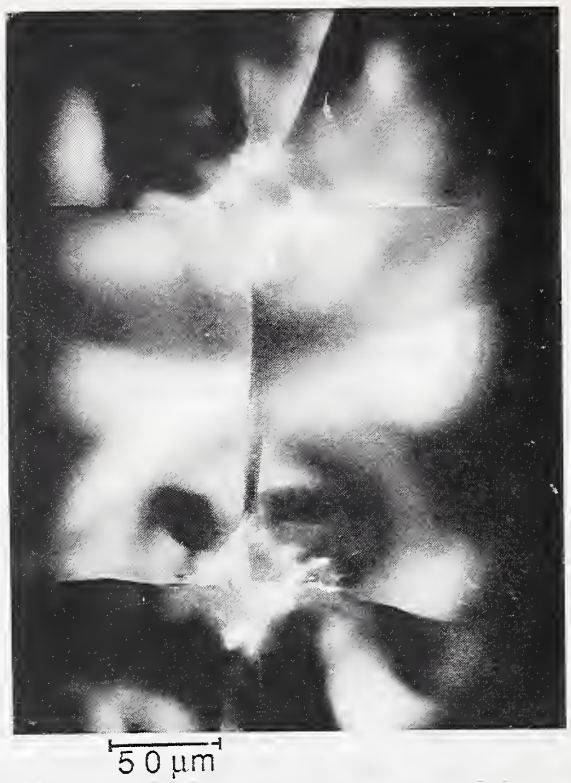

Figure 1. Optical reflection micrograph of a glass slide showing a Vickers indent pair and associated vertical and lateral cracks.

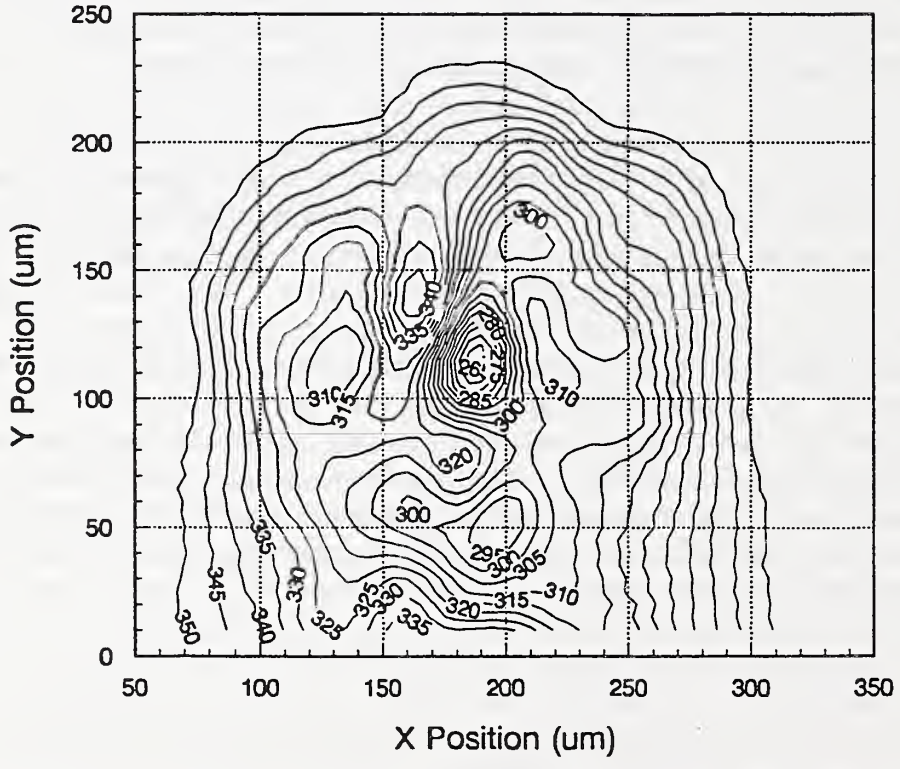

Figure 2. Ultrasonic echo-amplitude contour scan of the top portion of the Vickers indent pair in Fig. 1.

The distributed-damage samples were sintered reaction-bonded Si_3N_4 ceramics [4]. The effects of two levels of surface grinding, qualitatively termed "light" and "harsh" by industrial standards, were compared with "finely polished" material. The light grinding was representative of common industrial practice, while the harsh grinding consisted of "creep feeding" with a large depth of cut. The polish, light, and harsh grinding conditions generated distinct surface topographies of 0.04, 0.3, and 0.5 μm average roughness respectively, as determined by stylus measurements. All studies with normal-incident waves revealed a sensitivity of the ultrasonic echoes which appeared to be dominated by the surface roughness [5]. Efforts to focus beneath the surface resulted in echo signatures that again could be attributed to roughness rather than a difference in subsurface material structure. Finally, the amplitude of leaky surface waves revealed no distinguishing features that could not be ascribed to roughness.

The light- and harsh-ground samples were sectioned and polished for micrographic visualization [6]. The exposed subsurfaces revealed comparable features for the two samples, with the "damage" appearing to be commingled with only a slight extension of the surface topography. This is an indication that the depth of damage may be more significantly impacted by grain size, on the order of or less than ten micrometers for our fine-grained samples, than by grinding conditions such as these. As a result, we conclude that whereas the ultrasonic reflection technique is dominated by surface topography differences associated with these grinding conditions, this sensitivity to topography may itself be a meaningful delimiter of ceramic quality. A future research effort is to delineate the effects of subsurface damage and surface topography on our ultrasonic signatures. Controlled damage sites will be generated in ceramic samples and the effects of topographical features eliminated by overcoating or material removal.

REFERENCES

1. "International Conference on Machining of Advanced Materials," 20-22 July 1993, Gaithersburg, MD.

2. K. Yamanaka, Y. Enomoto, and Y. Tsuya, "Acoustic Microscopy of Ceramic Surfaces," IEEE Transactions on Sonics and Ultrasonics, SU-32, No. 2, 313-319 (1985).

3. Sample preparation and investigation by H. S. Ahn, visiting scientist from the Korean Institute of Science and Technology, Seoul, Korea.

4. Samples provided by T. J. Strakna and S. Jahanmir, Ceramics Division, NIST.

5. J. A. Slotwinski, N. N. Hsu, and G. V. Blessing, "Ultrasonic Measurement of Surface and Subsurface Structure in Ceramics," Proc. of the Intern. Conf. on Machining of Advanced Materials, 117-123 (June 1993).

6. Sample mounting and evaluation by L. C. Smith, Metallurg Division, and R. S. Polvani, Precision Engineering Division, NIST.

PUBLICATION

1. J. A. Slotwinski, N. N. Hsu, and G. V. Blessing, "Ultrasonic Measurement of Surface and Subsurface Structure in Ceramics," Proc. of the Intern. Conf. on Machining of Advanced Materials, 117-123 (June 1993).

Thermal Wave Investigation of Machining Damage

Grady White (301-975-5752), Lanhua Wei, and Said Jahanmir
Ceramics Division, Materials Science and Engineering Laboratory

The long range goal of this work is to develop a nondestructive evaluation (NDE) technique that will provide a parameter of machining damage that can be quantitatively related to the quality of the finished surface. The specific goals for this year were 1) to obtain baseline data relating machining processes to effective thermal diffusivity and 2) to adapt current thermal wave hardware and software to achieve state-of-the-art capabilities.

Machining has long been recognized as a major source both of defects in and expense of ceramic components. Many of the properties of ceramics which make them attractive in structural and chemical environments, e.g., high strength and chemical stability, make them difficult and time-consuming to machine. Additionally, the brittle nature of ceramics means that flaws generated by the machining processes frequently are the strength-limiting defects in the finished product. Traditionally, there has been a trade-off in the machining of ceramics; higher cutting rate and feed speed to reduce machining time in competition with low cutting rate and feed speeds for minimum flaw production. However, this trade-off has been based upon intuition rather than a scientific understanding of material responses to different machining parameters. In the Ceramics Division, there is a program underway as part of the Machining Consortium to study machining of ceramics to determine how the process can be optimized. This program includes investigating such parameters as cutting rates and loads, lubricants, etc. The ceramics will be characterized by various techniques to evaluate the effects of the machining processes; strength tests and nondestructive evaluation methods will form the core of the characterization.

The experimental technique we used during the past year, mirage thermal wave measurements, can be used to detect changes in thermal properties, either in line scans or in area images, or to evaluate thermal diffusivity. The technique involves heating the sample surface with a focussed, amplitude-modulated laser beam. The heated region, in turn, heats the adjacent atmosphere, generating a gradient in the index of refraction. A probe laser beam passed through the heated atmosphere is refracted and the amount the probe beam is deflected is measured by a position sensitive detector.

Because heat flow is affected by defects such as cracks, microcrack networks, densification, and vitrification, and because these features can all result from machining, both at the surface and beneath the surface, the measured thermal diffusivity is a natural parameter by which machining damage can be quantified. In addition, because thermal wave (TW) techniques provide surface and near-surface information and because the depth over which the information is obtained can be varied, thermal waves provide an ideal method for evaluating thermal diffusivity in the vicinity of the machined surface. We have demonstrated previously [1] that measurements of thermal diffusivity are sensitive to the grit size used in

grinding and that thermal waves can detect residual grinding damage even in specimens that exhibit no indications of damage optically. This work was aimed to extend these TW measurements to determine the effective thermal diffusivity of machined ceramics as a function both of distance from the surface as well as of machining parameters, and to relate the measured diffusivity both to other NDE techniques, e.g., ultrasound and capacitive probe measurements, as well as to destructive strength tests.

During the past year, we upgraded the mirage thermal wave system in the following manner. The system geometry was modified to allow the probe beam to reflect off, rather than to pass over, the specimen surface. This modification permits us to vary the separation between the specimen surface and the probe beam continuously from very small to very large values, by varying the distance between the point at which the probe beam strikes the surface and the point at which it intersects the heated region; this in turn allows modulation frequencies of tens of KHz to be used rather than the 3 KHz which was the previous upper limit. Because the penetration depth of the thermal wave signal is proportional to $f^{-1/2}$, where f is the modulation frequency, this improvement permits us to interrogate much thinner layers of material. A second improvement in the system was the inclusion of a second lock-in amplifier; the two lock-in amplifiers permit measurements of the deflection of the probe beam to be made in two orthogonal directions simultaneously. These two sets of data provide all the information needed for a 3-D analysis of the thermal properties of the surface to be obtained in one run. Finally, analysis software developed at Wayne State University was supplied to NIST to evaluate thermal diffusivity values. This software evaluates the thermal wave signal to provide information on the thermal diffusivities of film and substrate in multilayer systems, as well as estimates of film thickness. This type of analysis is being used to interpret machining effects in terms of a thin layer, in which the material is modified by the machining processes, and a bulk, unperturbed, substrate.

In addition to making improvements to the mirage system, we measured all of the silicon nitride machined specimens that we received as part of the machining program. We are also attempting to correlate these results with strength and ultrasonic measurements that other investigators are making on the same specimens. We determined that there appears to be an effective "film", i.e., a layer of material with modified thermal properties, on the surfaces of the machined specimens and that the thickness of these layers depends upon machining conditions. The physical meaning of this layer is presently under investigation. Similarly, measurements of the phase of the thermal wave signal (essentially a measure of delay time of the signal), were made for silicon nitride from different sources and with different machining conditions.

At this time, we detect no systematic relationship between measurement results and the machining process. Silicon nitride specimens from different sources appear to have surface layers that correlate differently with different measurements. For example, the phase shift measurements of the CERALLOY 147-3 specimens showed a correlation with volumetric removal rate of material and not with residual surface roughness. Measurements of effective thickness of residual machining damage in CERALLOY 147-3 ranged from 15 to 45

micrometers and appeared to be independent of the effective thermal diffusivity of the layer, which ranged from 0.38 to 0.46 cm^2/s. Similar measurements made on NORALIDE NBD-200 silicon nitride specimens produced damage layer thickness values of 3 to 4 micrometers with thermal diffusivity values of 0.16 cm^2/s. One difficulty in evaluating the thermal wave results of the machined specimens is that the damage caused by machining is extremely complex and the variations in damage generated in silicon nitrides of different grain sizes and glassy phases complicates the situation even more, making a clear picture difficult to obtain. Another difficulty is that the actual form of the damage generated by the different machining treatments is not well known. Therefore, interpreting the thermal wave signal in terms of specific damage formation is not possible.

In order to address these problems and to develop a better understanding of the thermal wave signals that result from machining damage, we recently begun to investigate damage generated by cyclic loading of ceramics. This damage, generated by subjecting a specimen to localized mechanical loading by a hard sphere, is expected to be a simpler version of the damage that might be generated beneath a surface subjected to wear. The thermal wave investigation of the specimens is a small part of a larger program led by Brian Lawn in the MSEL; guest scientists working with Dr. Lawn prepare the specimens and characterize the damage by optical and electron microscopy. Therefore, the extent and type of damage are well known before we look at the specimens, making it easier to interpret the thermal wave signals from the damage zone. Preliminary measurements were made on a glass ceramic and on a fine grained ($< 1\mu m$) silicon nitride and detected damaged regions, but detailed studies are just beginning.

During the past year, we maintained close contact with the consortium on machining which is headed by Said Jahanmir at NIST. The machining techniques which generated the specimens we investigated have been techniques under investigation by the consortium for applicability in the ceramics industry.

REFERENCE

1. G. S. White, "TW Investigation of Modern Ceramics," Proceedings of the CUICAC Workshop on NDE of Advanced Ceramics, Toronto, Canada (11/7/91).

PUBLICATION

1. Wei, L. and White, G. S., "Thermal Wave NDE of Advanced Materials Using Mirage Effect Detection," Proceedings of "Review of Progress in Quantitative NDE," submitted to Plenum Pub. Co., 1993.

Depth of Case-Hardening

A. H. Kahn (301-975-6146) and L. C. Phillips
Metallurgy Division, Materials Science

E. Lagergren (301-975-3245)
Statistical Engineering Division, Computing and Applied Mathematics Laboratory

K. White, Guest Worker
Saginaw Division, General Motors Corporation

This report represents the conclusion of the empirical study of eddy current methods for the determination of the depth of case hardening of automotive steel drive axles. The research was carried out jointly by NIST and General Motors under a Cooperative Research and Development Agreement (CRADA). The objective of this project has been to obtain the ultimate accuracy of the case depth measurement using the nondestructive eddy current measurement. A description of the method in this application was given in the 1992 report of this series [1]. The tests we report were conducted on 72 case hardened steel drive shafts, all of nominal dimensions 2.54 cm (1 in.) in diameter and 30.48 cm (1 ft) in length. The samples were measured by the electromagnetic method, and subsequently the hardness was determined by destructive sectioning. The depth of case hardening was defined, in this application, as the depth beneath the surface at which the hardness decreased to Rockwell 50. For each of 3 heats (steel preparations), samples were treated according to process schedules to produce 8 nominal depths of case hardening, from 3.2 mm to 5.6 mm, with 3 samples for each depth (72 samples in all). Electromagnetic measurements, and later, microhardness profile measurements following destructive sectioning, were made at three locations on each shaft (two near milled grooves, and one at a smooth site). Thus 216 individual measurements were performed.

We examined the result statistically and found, combining data over all heats and locations, that the characteristic electromagnetic response that best correlated with destructively measured case depth was the magnitude of the peak real part of the normalized impedance. The standard deviation of case depth when using the magnitude of this peak was 0.31 mm.

For a fixed heat and fixed location, one would expect less statistical spread. Under these conditions, the characteristic that best correlated with destructively measured hardness was the real part of the normalized impedance at 10 Hz. The standard deviation of case depth when using this characteristic was 0.22 mm. (For fixed heat and location, and using the earlier magnitude of the peak as the characteristic, the standard deviation was found to be 0.24 mm.)

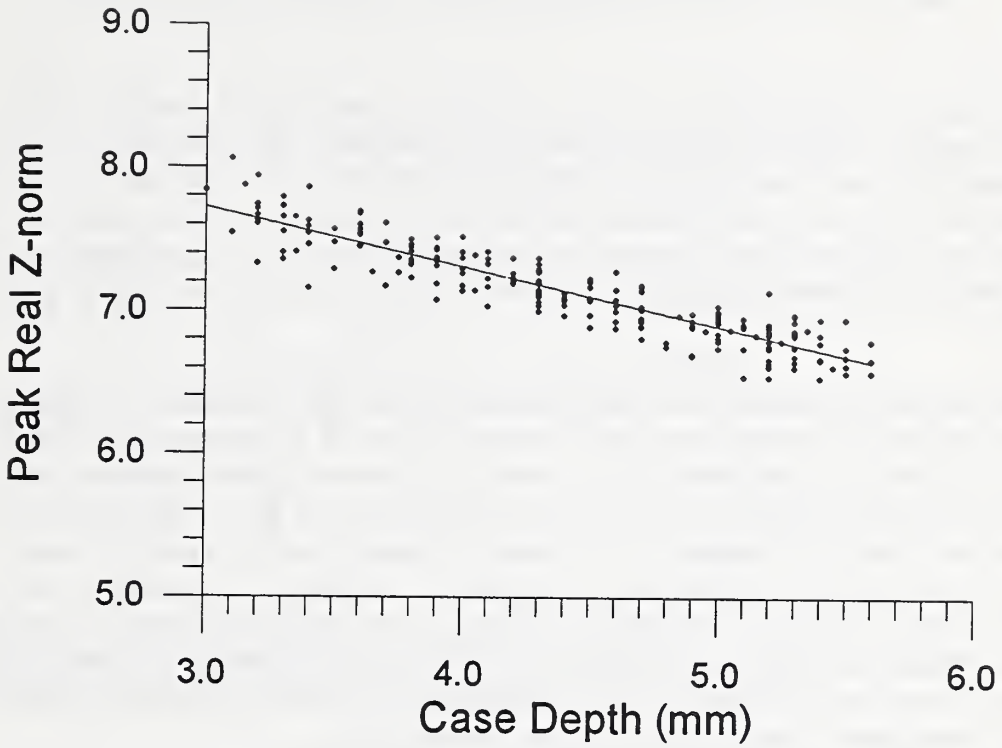

Fig. 1. Plot of measurements of the magnitude of the real part of the normalized impedance as a function of the destructively measured case depths. All 216 measurements from the samples of 3 heats and at 3 site locations are included.

The results of this project are now being compared with those of acoustic methods. Additional studies on the effects of ferromagnetism on the interpretation of eddy current measurements are continuing.

REFERENCE

1. A. H. Kahn, L. C. Phillips, D. Lu, and K. White, "Depth of Case Hardening," in Intelligent Processing of Materials, Technical Activities 1992, NSTIR 4963, pp.44-45.

Aluminum Temperature Measurement

A. H. Kahn (301-975-6146) and L. C. Phillips
Metallurgy Division, Materials Science and Engineering Laboratory

A definitive test of the Eddy Current resistivity and temperature sensing system, developed under a CRADA with The Aluminum Association, Inc., with construction and installation by the Data Measurement Corporation, was executed. The test was performed at the Lancaster, PA plant of the Alumax Mill Products Corporation under conditions of normal production of rolled aluminum sheet for approximately one month. The objective was to monitor temperature during processing in order to maintain optimum quality of the finished product.

The eddy current system functions by using two solenoids positioned on opposite sides of the test material. One coil serves as a primary, driven at frequencies typically from 50 to 150 Hz and carrying a current of 20 A. A voltage is induced in the secondary coil; its magnitude and phase depend upon the resistivity and thickness of the sheet, and to a lesser degree on the speed of the material. Thickness is routinely obtained with an x-ray attenuation gauge. The measurement system obtains the electrical resistivity which, in turn, depends on the temperature. The details of obtaining the temperature from the resistivity, taking into account the effects of alloy composition, were discussed in the 1992 Report of Intelligent Processing of Materials [1]. A description of the equipment used and the resistivity measurement method was reported previously [2].

In preparation for this demonstration, a related test was performed at the Alcan Research and Development Centre at Kingston, Ontario. The objectives were to ascertain the magnitude of electromagnetic velocity effects, to perform simultaneous measurements of temperature with the eddy current instrument and an infrared pyrometer, and lastly, to determine whether there were significant metallurgical changes in samples of the aluminum collected before and after heating to rolling temperature.

At speeds up to 1.8 m/s (350 ft/min), no detectable electromagnetic effects arising from velocity could be detected. Figure 1 shows a typical speed run. The temperature reading is that given by the eddy current sensor.

Concurrent measurements of temperature by the eddy current method and by an infrared pyrometer are shown in Figure 2. The temperature of the aluminum sheet was varied by controlling the speed with which it passed through the furnace used for the heating. Speed is shown in the upper curve. At the higher temperatures the parallel tracking of the two sensors is excellent. However, there is an offset between the two readings of approximately 30°C that we cannot fully explain. We did find that the offset was sensitive to the elevation of aluminum sheet. This suggests the possible role of stray infrared radiation or focussing

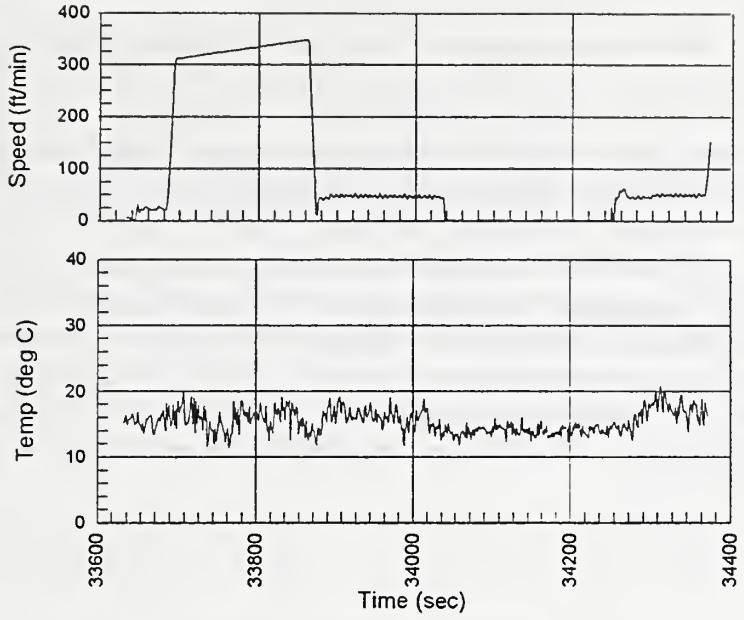

Fig. 1. Typical speed test; plots show speed and EC temperature readings. Note insensitivity of temperature reading to gross speed changes.

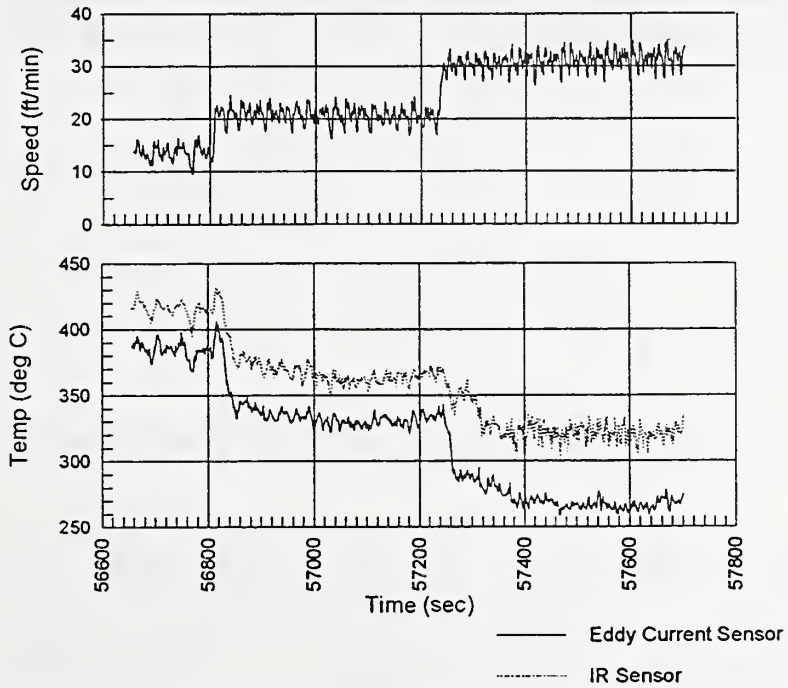

Fig. 2. Tracking of EC and infrared sensor readings. Temperature of moving aluminum sheet was controlled by speed through furnace.

effects in shifting the infrared reading. The lowest temperature was below the recommended range of the particular infrared sensor used.

The electrical resistivity of the samples that had been heated showed a typical drop of 0.06 microhm cm, which corresponds to an eddy current sensor drop of 6 °C. We presume that this reduction was caused by an annealing of deformation that occurred from the rolling during production. This is consistent with earlier laboratory work at NIST by A. Stern, in which heating to 400 °C for 2 minutes produced a drop in resistivity of 0.035 microhm cm.

In addition to the above preparations, carried out at Kingston, we have examined in our laboratory 50 samples of 3004 aluminum sheets taken from coils rolled from different ingots. These are typical of the material to be examined in the coming test. We observed an overall spread in resistivities corresponding to a temperature spread of +/-10 °C. This spread was dominated by the variations in resistivity associated with variations in the composition and metallurgical state of the 50 samples. The instrumental uncertainty and thickness uncertainty corresponded to only +/-3 °C each.

REFERENCES

1. A. H. Kahn, L. C. Phillips, "Eddy Current Temperature Sensing", Intelligent Processing of Materials, NISTR 4963, pp. 23-27, 1992.

2. M. Gvishi, A. H. Kahn, and M. L. Mester, "Eddy Current Testing of Carbon-Carbon Composites," Review of Progress in Quantitative Nondestructive Evaluation, Vol. 11, p. 289, edited by D. O. Thompson and D. E. Chimenti, Plenum Press, New York, 1992.

Eddy Current Liquid Metal Flow Rate Sensor

L. C. Phillips (301-975-5667) and A. H. Kahn
Metallurgical Sensing and Modeling Group, Metallurgy Division

The objective of this project has been to establish the feasibility of using an eddy current sensor in measuring the liquid metal flow rate during the production of metal powders. This effort is part of a greater effort of the NIST/Industrial Consortium on Automated Processing of Rapidly Solidified Metal Powders by High Pressure Inert Gas Atomization. The consortium focuses on the application of intelligent processing techniques using real-time controls in order to automate the process. The goal is real-time control of the process and production of particles with optimum size and size distribution. In the process, the liquid metal flow rate is an extremely important parameter that is not easily measured. This project explores the use of a non-contact eddy current sensor for that application.

The eddy current liquid metal flow rate sensor model is based upon the multi-turn three coil configuration shown in Figure 1. The system uses a central driving coil with two

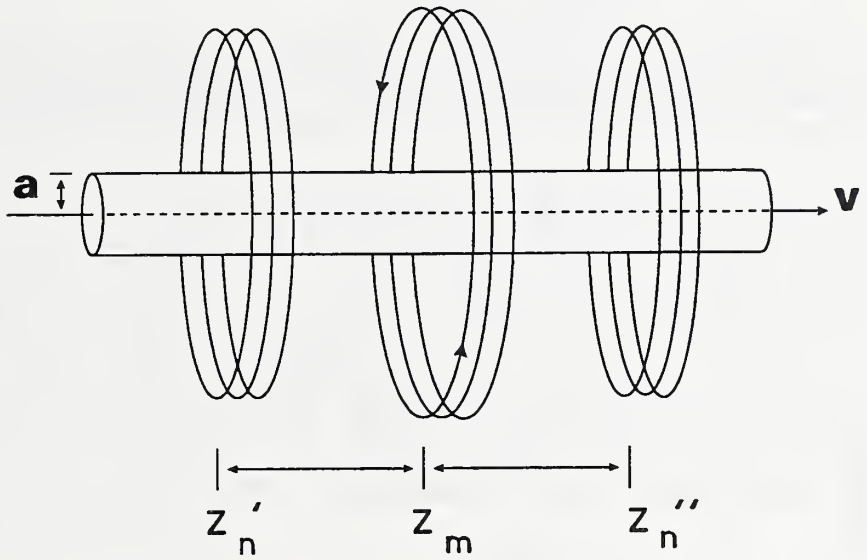

Figure 1. Schematic drawing of the three coil eddy current sensor.

identical sensing coils positioned symmetrically. If the sensing coils are wired in opposition, then a null voltage will be detected in absence of any fluid flow. When the material begins to flow, an induced voltage will develop that is proportional to the velocity and is dependent upon the electrical properties of the material. The calculations in determining the induced voltages are based upon solving the differential equation describing the magnetic field produced by an ac current loop surrounding a cylindrical moving rod.[1,2] An integral solution

in closed form has been obtained for this problem by Kahn and Phillips[3]. Both the distributed length of the coils and the non-uniform velocity profile have been accounted for in the theoretical model. The electrical properties can also be monitored independently from the velocity effects by switching the wiring of the sensing coils to the series configuration. In the series configuration, the induced voltage from the flow velocity is a higher second order effect and hence is negligible. This configuration can then be used to determine the electrical properties and the bore diameter. Switching between the sum and difference modes is not complicated.

For testing the eddy current sensor, a room-temperature laboratory mercury flow system has been constructed with geometric parameters similar to those in the NIST Atomizer system. A 6.35 mm (¼ in.) O.D. and 3.18 mm (⅛ in.) I.D. tube has been used to simulate the atomizer delivery tube with a gravity feed tank producing the intended flow rate. The eddy current sensor is comprised of a driver coil and two receiver coils each having 12 turns. The overall length of the eddy current sensor is approximately 15 mm. The maximum flow velocity achievable in the test system has been shown to be 1.25 m/s. Although the parameters for the laboratory and NIST Atomizer flow systems are not exactly the same, the theoretical model predicts a reasonable similarity for the sensor voltage response.

The resultant voltage outputs for two selected frequencies (100 kHz & 40 kHz) as a function of flow velocity are shown in Figures 2 and 3. The data were collected at a primary drive current of 1 Ampere. The solid lines in these two figures represent the

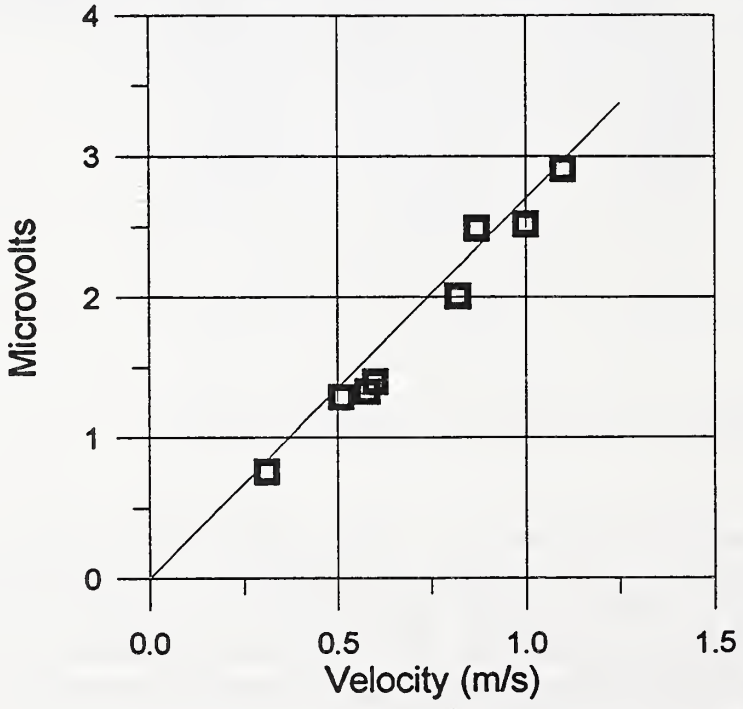

Figure 2. Eddy current response at 40 kHz using the Hg test flow system.

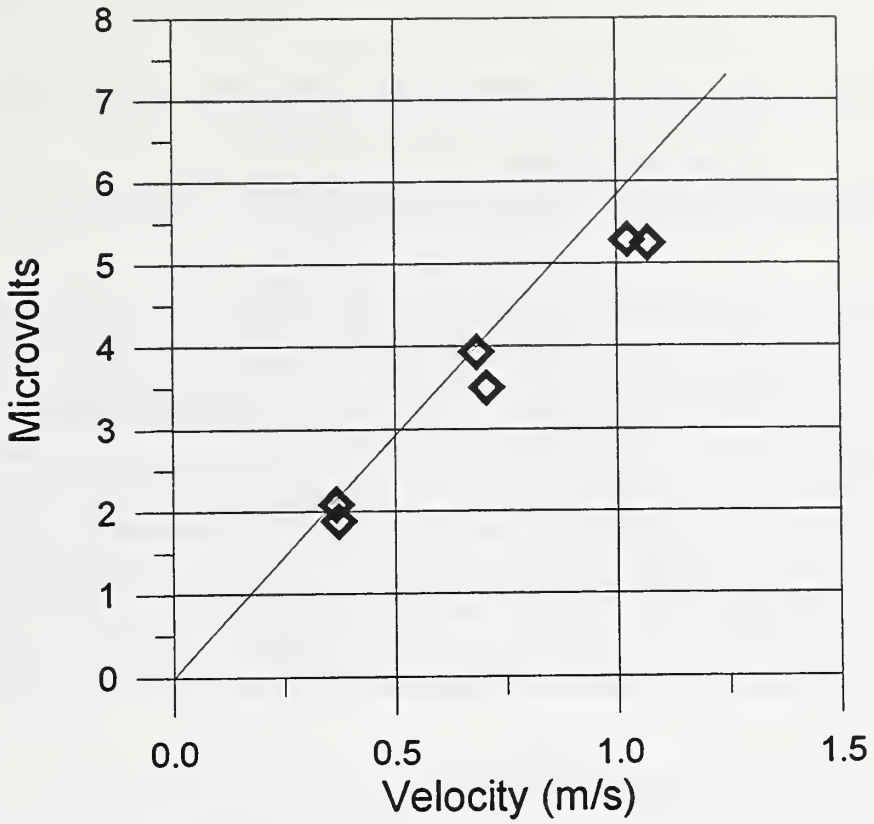

Figure 3. Eddy current response at 100 kHz using the Hg test flow system.

expected response from the theoretical model, with the data showing relatively good agreement. The model assumes a turbulent flow condition and uses an empirical relation, the Prandtl Power Law, to estimate the velocity profile based upon the Reynolds number of the flow condition. Examination of the frequency response at a constant velocity of ~1.0 m/s is shown in Figure 4. Again, the solid curves in this figure show the predicted model responses for different flow conditions with the experimental data overlaid. The optimum sensor response should occur at about 300 kHz; however due to a stray capacitance problem, this has not yet been experimentally achieved. Below 100 kHz, the data demonstrated good agreement with the model. When operating at 100 kHz, the signal-to-noise ratio (SNR) for the sensor was found to be 30.

To date, the eddy current flow velocity sensor has demonstrated the ability to detect flow velocities that would be seen in the equivalent Metal Atomization system. The output voltage is indeed linear with velocity and the sensitivity approaches that needed for a viable sensor technique. However, there are still several discrepancies between the model and the reported sensor response that need to be resolved. Progress on these fronts includes further refinement of the sensor to address the stray capacitance problem, and developing a high temperature flow test.

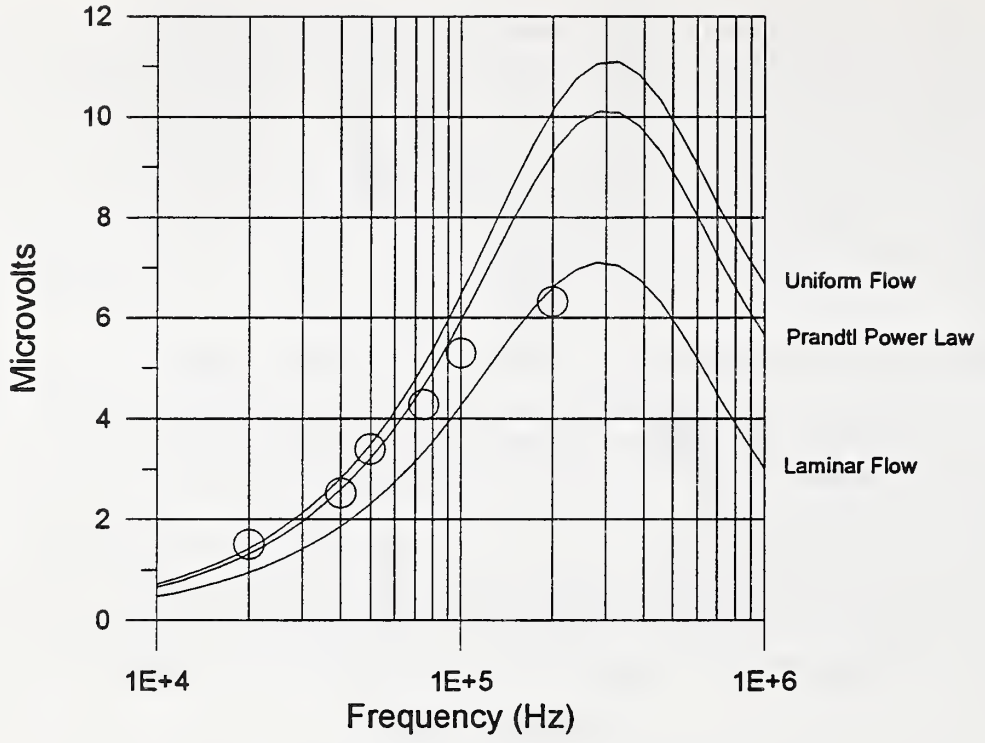

Figure 4. Eddy current response as a function for a flow velocity of 1 m/s.

REFERENCES

1. C. V. Dodd and W. A. Deeds, "Analytical Solutions to Eddy-Current Probe-Coil Problems," J. Appl. Phys. **39**:2829 (1968).

2. C. C. Feng, W. E. Deeds, and C. V. Dodd, "Analysis of eddy-current flowmeters," J. Appl. Phys., 1975, **46**, 2935-40.

3. A. H. Kahn and L. C. Phillips, "Development in the Theory and Analysis of Eddy Current Sensing of Velocity in Liquid Metals," J. Nondestr. Eval., Vol. 4, Issue 4, 237-24.

Monitoring of Sheet Metal Rolling with Combined Laser/EMAT Sensors

J. B. Spicer and G. A. Alers (301-975-6140)
Metallurgy Division, Materials Science and Engineering Laboratory

Many processing steps in steel and aluminum mills take place at elevated temperatures and on materials that are moving very rapidly past the sensor. A particularly good example of this is in the rolling of copper and brass sheet metal, where the texture and grain size of the final product are controlled by deformation and annealing steps performed under strict control at elevated temperatures. Since both EMAT and laser ultrasonic sensors have non-contact characteristics that should enable them to meet these on-line monitoring requirements, a preliminary study was undertaken to determine the optimum combination of these two sensors for application to the rolling of copper and brass. By configuring a future process monitoring system around a laser source of sound and an EMAT detector, the ease of generating high amplitude ultrasonic waves optically can be combined with the simplicity and mode selectivity of EMAT detectors even though the latter may have to be mounted close to the moving sheet.

Other studies within the Metallurgy Division have demonstrated that a Laser source and an EMAT receiver could make simultaneous measurements of the sound velocity of both the symmetric and antisymmetric Lamb wave modes even when the sheet was moving past the sensor at a speed of 35 m/s (6900 ft./min). The literature shows that the anisotropy in the velocity of the symmetric mode can be used to specify the texture and that the decrease in amplitude of any specific mode as a function of travel distance can be used to measure the ultrasonic attenuation coefficient and hence the grain size in the material. In order to verify that these measurement principles could be applied to copper and brass, a suite of samples with different textures and grain sizes was provided by the Olin Corporation. A laser transmitter and a single mode EMAT receiver were assembled to measure the velocity of the symmetric Lamb wave mode as a function of angle relative to the rolling direction. A pair of high frequency, single mode EMATs were used to measure the attenuation coefficient of a 3.2 MHz Lamb wave mode in brass samples with grain sizes between 20 and 100 μm. The results are shown in Figures 1 and 2, which show clearly that the texture (as betrayed by the shape of the sound velocity versus angle curve) is very sensitive to heat treatment and composition and that different grain sizes in brass can be easily distinguished by the rate of decrease of the amplitude of the 3.2 MHz Lamb wave as a function of distance traveled.

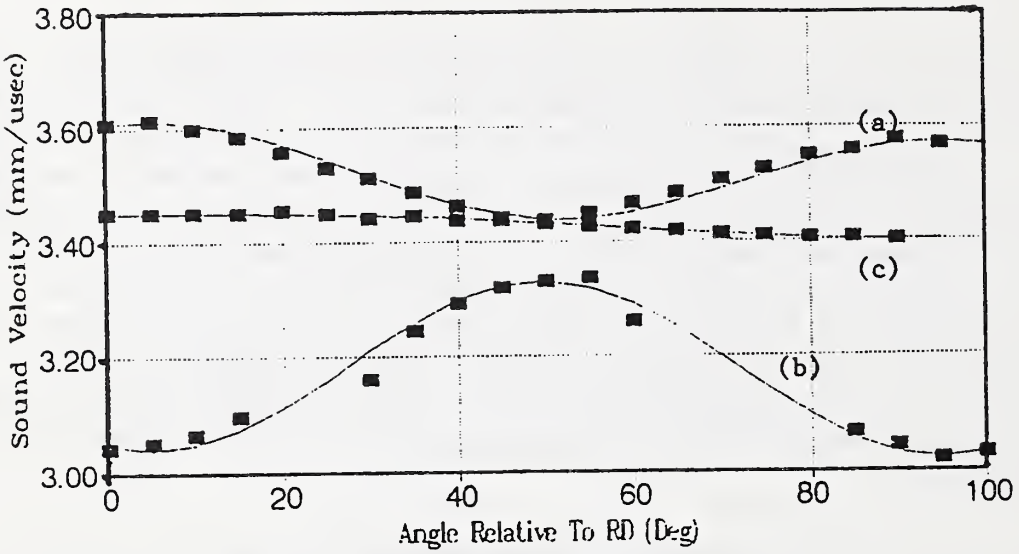

Figure 1. Angular dependence of the velocity of the S_o Lamb wave mode in (a) as rolled copper, (b) annealed copper and (c) cold rolled brass.

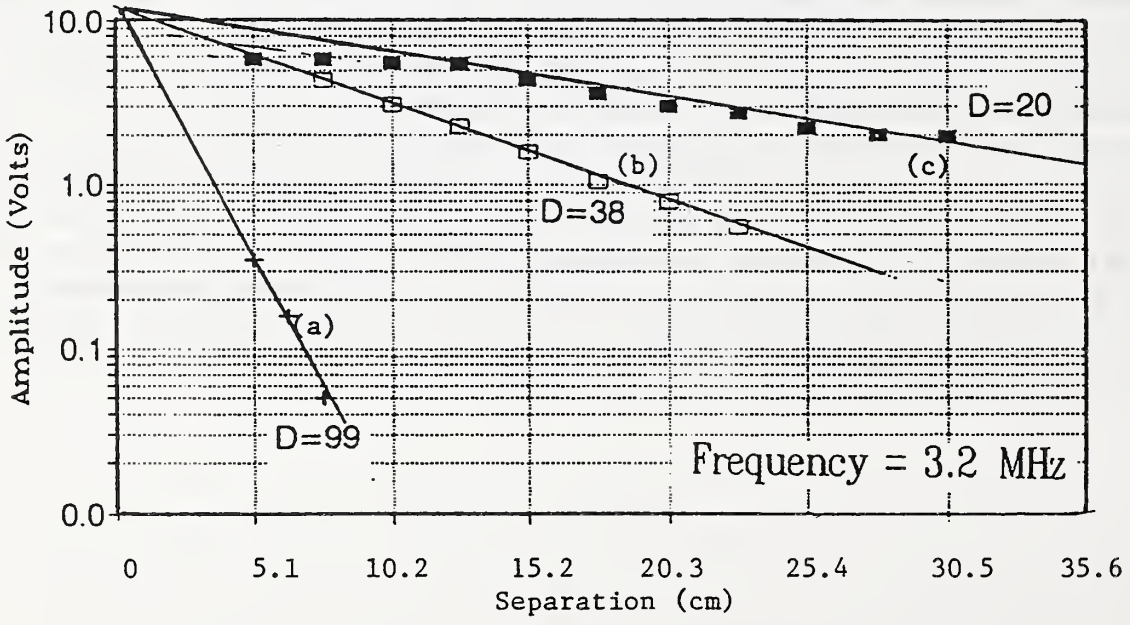

Figure 2. Amplitude of a 3.2 MHz Lamb wave as a function of distance traveled in brass with different grain sizes. (a) 99 μm, (b) 38 μm and (c) 20 μm.

Sensor for Measurement of Microstructure in Hot Steel

A. V. Clark (303-497-3159), M. G. Lozev, and B. J. Filla
Materials Reliability Division
Materials Science and Engineering Laboratory

Under the auspices of the American Iron and Steel Institute, NIST recently began research on microstructural engineering for hot strip mills. The goal is development of computer models to allow prediction of microstructure and mechanical properties, given input chemistry and mill history.

A companion program has also been initiated (with NIST funding) on a first generation of sensors for microstructure evolution. Such sensors have utility because: 1) they can be used to verify predictions of microstructure models in a nondestructive fashion; 2) they could ultimately be incorporated in an intelligent processing system. Here, sensor outputs would be used as inputs to a process control system. If the microstructure (as measured by the sensor during processing) is "drifting" from desired values, the system would choose a "best" strategy for changing mill parameters to achieve the desired microstructure.

In the current project, a sensor is being designed to measure austenite grain size during hot rolling of steel plate. Austenite grain size prior to transformation determines the subsequent ferrite grain size, which, along with chemistry, is a determinant of mechanical properties. Thus it is important to monitor the austenite grain size during hot rolling to insure that it has the desired value.

The classical method of measuring grain size nondestructively is by attenuation of ultrasonic waves. In a plane wave, the amplitude decay due to attenuation is given by $\exp[-\alpha x]$ where x is propagation distance and α is the attenuation coefficient. Part of the attenuation of waves passing through a polycrystalline material is due to scattering of sound by the grains. When the wave length is much larger than the grain size theory predicts an attenuation coefficient due to scattering given by [1]:

$$\alpha_{sc} = A[2V_L^{-5} + 3V_s^{-5}]f^4T$$

where A depends on density and the elastic moduli, f = frequency, V_L and V_s are longitudinal and shear wave velocities and T has units of volume. If all the grains are the same size, d, then $T = 4/3\ \pi d^3$.

At room temperature, attenuation is also affected by other (anelastic) effects. These have a different frequency dependence than α_{sc} so it is necessary to measure attenuation at multiple frequencies (e.g. over a decade) and extract the f^4 component to determine grain

size. However, at elevated temperatures in hot rolling, α_{sc} is expected to be dominant; the required frequency range may only be an octave.

Attenuation measurements at elevated temperature are more difficult to perform. Because the velocity of sound decreases with temperature, the attenuation coefficient will be several times larger at 1000 °C. This presents a signal-to-noise problem; at high frequencies, it will be difficult for sound to penetrate hot steel. This is especially true in hot-rolling, where plate thicknesses are typically in the range 30-50 mm. Large losses and high frequencies in thick specimens preclude the use of techniques such as laser-generated ultrasound.

Also, injecting sound into the plate requires special consideration. Most conventional ultrasonic transducers become inoperative (lose their piezoelectric property) at temperatures above several hundred degrees centigrade. The acoustic couplants normally used to couple sound from transducer to specimen are inoperative at high temperatures and leave a residue on the specimen surface.

In hot rolling, there will be interpass times where the plate is at rest; it is possible to have momentary contact to inject an ultrasonic signal. This can be done by a buffer rod. One end of the rod will be forced onto the surface of the plate and a piezoelectric crystal is mounted on the other (cool) end. The buffer rod protects the crystal from the harsh environment at the plate surface where temperatures can be of order 1000 °C. It will be necessary to press the buffer rod onto the specimen with sufficient force to achieve ultimate metal-to-metal contact. This occurs when the asperities due to surface roughness of specimen and buffer rod "flatten out" sufficiently to allow sound transmission.

A facility to simulate attenuation measurements in steel plate during hot rolling is now being constructed. A photograph of the major components is shown in Figure 1. The system consists of: a custom-made furnace to heat specimens to 1000 °C; steel specimens with known grain size; a buffer rod; hydraulics to press the buffer rod onto the specimen; transducer and associated electronics to generate and receive ultrasonic waves.

The system operation is envisioned as follows: under computer control, the hydraulics will force the buffer rod down onto the sample with sufficient force to achieve intimate metal-to-metal contact. Then sound generated by the transducer can propagate down the buffer rod and be partially transmitted into the specimen. The sound transmitted through the buffer rod-specimen interface will reflect from the "backwall" of the specimen and return to the transducer by way of the buffer rod. This (B) echo plus the (A) echo from the partial reflection at the buffer rod-specimen interface will be amplified by the electronics for subsequent data reduction.

In attenuation measurements there are 3 unknowns: the amplitude of the signal generated by the transducer; the amount of reflection of sound at the buffer rod-specimen interface; the attenuation in the sample. All of these influence the amplitude of the reflected

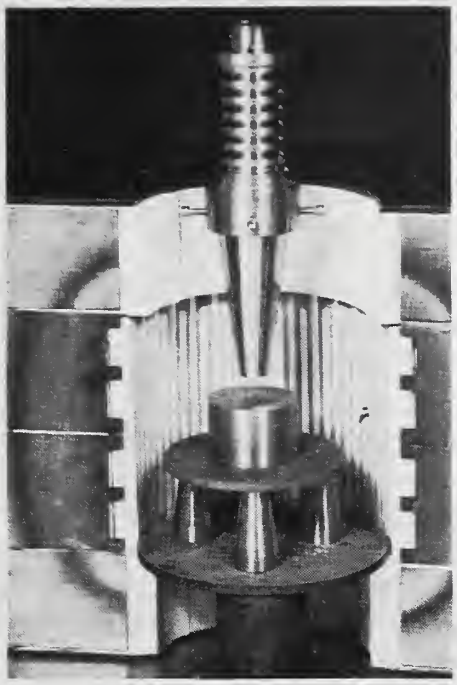

Figure 1. Photograph of system for simulation of grain size measurement in hot rolling. Door to furnace has been opened to show sample being contacted by buffer rod. On top of buffer rod is cooling jacket/anwaves. Thus the amplitude of 3 waves must be measured: the third is the (A') echo from the end of the buffer rod just before contact with the specimen.

waves. Thus the amplitude of 3 waves must be measured: the third is the (A') echo from the end of the buffer rod just before contact with the specimen.

In a rolling mill, plastic deformation of the plate surface on the order of a mm causes no significant problems. However, because we wish to use our samples repeatedly, we must avoid such plastic deformation. At elevated temperatures the yield stress decreases with strain rate and is much lower than at ambient temperature. Manual control of the mechanical testing machine will cause plastic deformation of the specimen surface and degrade coupling of sound from buffer rod into specimens. Hence, we are implementing a computer program that will cause a rapid loading of the specimen by the buffer rod to a stress just below the yield stress, and then the specimen will be slowly unloaded. During unloading the A and B echoes will be measured: when the sample is completely unloaded the A' echo will be measured. This loading/unloading cycle will be repeated many times to allow measurements of attenuation at different frequencies.

The buffer rod will apply stress to the specimen surface. We require a buffer rod material that is mechanically stable under loads at elevated temperatures. At elevated temperatures, the mechanism of plastic deformation is motion of grain boundaries. Typical materials for high temperature applications are coarse-grained; these would cause excessive attenuation of sound waves in the buffer rod, degrading the signal-to-noise ratio in attenuation measurements. The buffer rod material we selected is a nickel-based alloy that has a 0.5 μm grain size, good mechanical properties to at least 1150 °C, and is oxidation resistant. Its recrystallization temperature is about 1350 °C, so grain growth during our experiments will not occur.

A cooling jacket/anvil is placed between the load cell in our mechanical testing machine and the buffer rod. This protects the load cell and hydraulics from heat conducted up the buffer rod. The cooling jacket/anvil has good thermal conductivity and is strong enough to transmit the required load to the top of the buffer rod. A recess has been machined into the bottom of the cooling jacket to allow placement of the ultrasonic transducer.

The transducer is a critical component, since it should operate at temperatures around 200°C, the expected environment on top of the buffer rod. Also, it should have wide bandwidth. The center frequency of the transducer is chosen to optimize precision of measurement of attenuation. An error analysis showed that for given signal-to-noise ratio, best precision will be obtained when $B/A = e^{-1}$; i.e., the backwall echo is e^{-1} times the reflected echo, A. This occurs when $2\alpha_{SC}L = 1$, where L = specimen thickness. Specimen thickness, grain size, and the temperature dependence of moduli and density are known; we calculated the optimum center frequency from equation (1) to be about 5 MHz.

Our multi-element transducer consists of a gold foil placed on the buffer rod, a piezoelectric crystal (lithium niobate) on top of the foil, a silver foil electrode on top of the transducer, a roughened brass plate on top of the silver foil, a compliant material, and a stainless steel plate. Lithium niobate was chosen for the crystal material since it can operate at several hundred degrees centigrade. Its acoustical properties are also close to that of the buffer rod.

The transducer assembly is pressed down onto the buffer rod by a bolt. This bolt-loading causes acoustic coupling so that the forward-travelling sound wave generated by the crystal travels through the gold foil and into the buffer rod. Backward-travelling waves are transmitted through the silver electrode into the brass, where the roughened back scatters the sound to increase acoustic bandwidth. The frequency response has been modeled with results shown in Figure 2. Because the acoustic properties of the crystal, buffer rod, silver foil, and brass are close to each other, and because the gold foil is thin, the transducer has a broad frequency response.

Also shown in Figure 2 is the theoretical response of a second transducer being built to our specifications. It consists of a lithium niobate crystal brazed to a buffer rod with an aluminum-magnesium compound. Because the compound has different acoustical properties

from the crystal and buffer rod, and because brazing requires relatively large thickness (0.2 mm) this transducer will have less bandwidth. However, commercial transducers based on this brazing concept have been subjected to many thermal cycles in field applications (e.g. monitoring the integrity of pressure vessels at elevated temperatures). Hence this design has the advantage of proven reliability in ruggedness. We will test the merits of both transducer designs in future work.

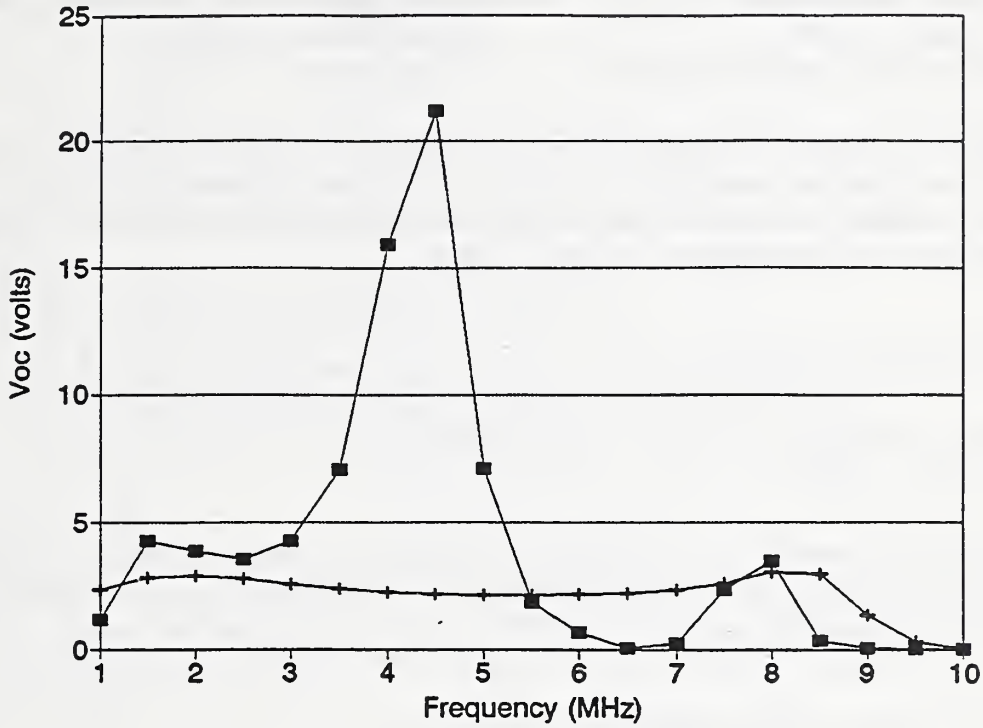

Fig. 2. Theoretical calculations of frequency response of 2 transducer designs; + = multi-element design with pressure plate; ▪ = transducer with lithium niobate brazed to buffer rod.

REFERENCE

1. A. B. Bhatia, "Scattering of High-Frequency Sound Waves in Polycrystalling Materials," J. Acoust. Soc. Am. 31, p. 16, (1959).

PUBLICATION

1. A. V. Clark, M. G. Lozev, B. J. Filla and L. J. Bond, "Sensor System for Intelligent Processing of Hot-Rolled Steel," presented at the Sixth International Symposium on Nondestructive Characterization of Materials, Oahu, Hawaii, June 7-11, 1993, to be published.

PERSONNEL

The permanent staff of the Office of Intelligent Processing of Materials is listed below.

OIPM PERMANENT STAFF IN FISCAL YEAR 1993

H. Thomas Yolken, Chief*
Deputy Chief, Vacant*
George Birnbaum, Senior Scientist*
Patty Salpino, Administrative Officer
Ellen Altman, Secretary
Linda Souders, Secretary

*In the absence of a Deputy Chief, Dr. Robert Schaefer of the Metallurgy Division, has been serving as a part-time staff member since October 1992. Since February 24, 1992, Dr. George Birnbaum has assumed some of the duties of the Deputy Chief. Dr. Dale Hall joined the office as the new chief on March 21, 1994.

A. OIPM SEMINARS AT NIST

Nagendra Palle, University of Illinois, "Adaptive Mesh Refinement for Solidification Problems," April 2, 1993.

J. F. de Belleval, Université de Technologie de Compiégne, France, "Acoustic Propagation in Anisotropic Periodically Multilayered Media, Floquet Waves Permit to Solve Numerical Instabilities," July 27, 1993.

B. INVITED TALKS AND PAPERS BY OIPM STAFF

Overview of the Materials Science and Engineering Laboratory, H. T. Yolken, NIST, Boulder, Colorado, March 18, 1993.

"Intelligent Processing of Materials," G. Birnbaum, COMAT NDI/E Task Group Meeting, Institute for Defense Analysis, Alexandria, VA, July 13, 1993.

"Cancellation Effects in Collision-Induced Phenomena," G. Birnbaum and B. Guillot, NATO Advanced Research Workshop on Induced Spectroscopy: Advances and Applications, Banff Center for Conferences, Banff, Alberta, Canada, August 30, 1993.

"Transmission Properties of Window Regions of the υ_4 Band of Methane," M. E. Thomas and G. Birnbaum, The Second Symposium on Research and Development at Applied Physics Laboratory, Johns Hopkins Applied Physics Laboratory, Laurel, MD, November 2, 1993.

PUBLICATIONS

"Collision-Induced Absorption in Mixtures of Symmetrical Linear and Tetrahedral Molecules: Methane-Nitrogen," G. Birnbaum and A. Borysow, J. Chem. Phys. 99, 3234-3243 (1993).

D. COMMITTEES, CONFERENCES, AWARDS AND APPOINTMENTS

H. Thomas Yolken

William P. Slichter Award for outstanding collaborative research in support of supersonic inert gas metal-atomization consortium
Executive Committee and Board of Directors, American Society for Nondestructive Evaluation
Editor-in-Chief, Research in Nondestructive Evaluation
ASM - Heat Treatment Steering Panel
Co-chairman Second ASNT Research Symposium on NDE
Program Committee, Eighth International Forum on New Materials, Italy

George Birnbaum

Associate Editor, Research in Nondestructive Evaluation
Chairman, Session on Metals Processing, ASNT Second Annual Research Symposium on NDE for Process Understanding, Sensing and Control, Nashville, Tennessee, March 30, 1993.

National Institute of Standards and Technology

Organizational Chart

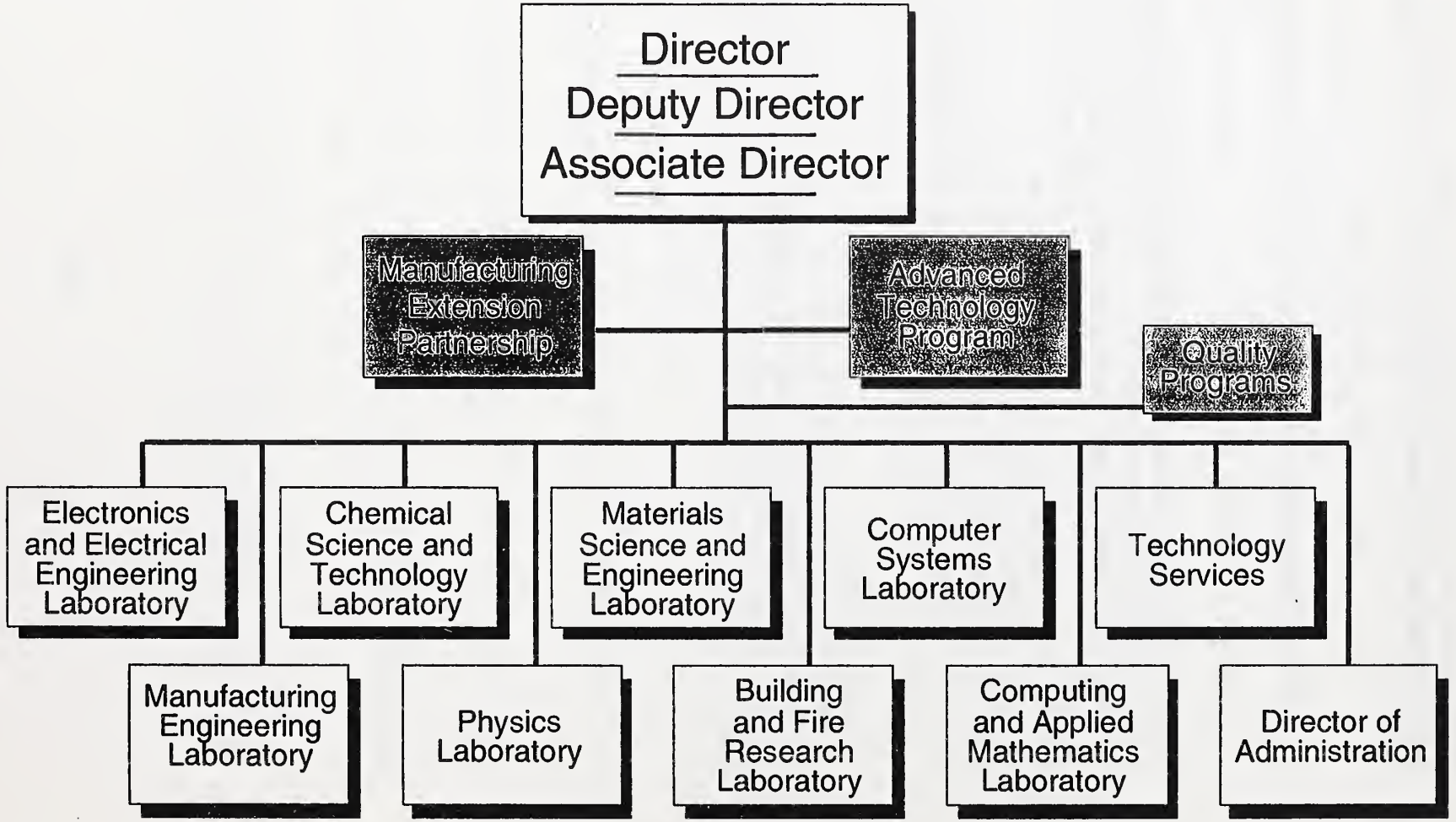

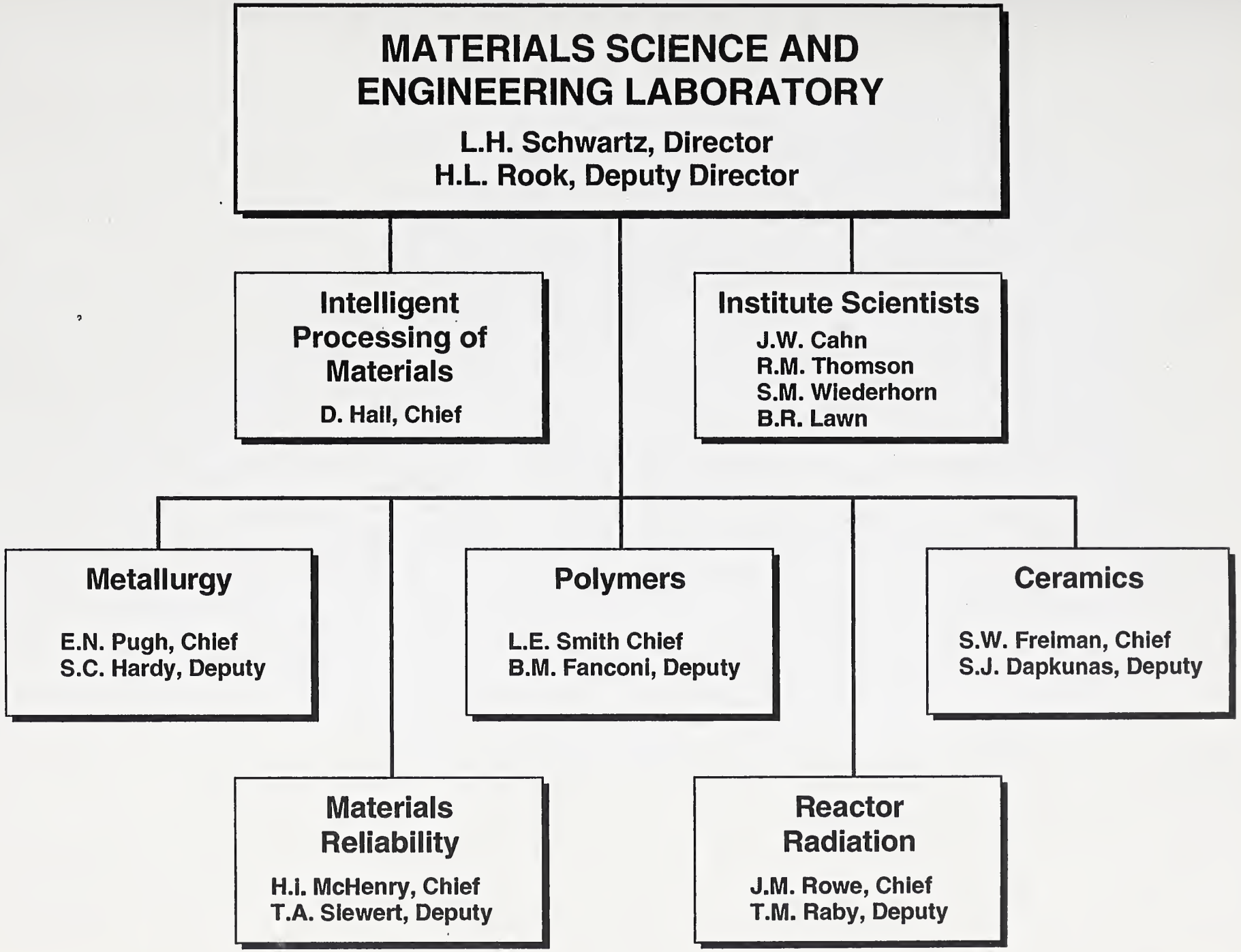
MATERIALS SCIENCE AND ENGINEERING LABORATORY
L.H. Schwartz, Director
H.L. Rook, Deputy Director
Intelligent Processing of Materials
D. Hail, Chief
Institute Scientists
J.W. Cahn
R.M. Thomson
S.M. Wiederhorn
B.R. Lawn
Metallurgy
E.N. Pugh, Chief
S.C. Hardy, Deputy
Polymers
L.E. Smith Chief
B.M. Fanconi, Deputy
Ceramics
S.W. Freiman, Chief
S.J. Dapkunas, Deputy
Materials Reliability
H.I. McHenry, Chief
T.A. Siewert, Deputy
Reactor Radiation
J.M. Rowe, Chief
T.M. Raby, Deputy